Fine Chemical Engineering
https://ojs.wiserpub.com/index.php/FCE/

Research Article

# The Co-Biosorption Possibility of Single and Quaternary Heavy Metals by Multi-Metal-Tolerant Bacteria Isolated from Electroplating Effluents

**Eeman Alhammadi*, Normala Halimoon, Zufarzaana Zulkeflee, Wan Lutfi Wan Johari**

Department of Environment, Faculty of Forestry and Environment, Universiti Putra Malaysia, 43400, UPM Serdang, Selangor Darul Ehsan, Malaysia
E-mail: e.alhammadi@uot.edu.ly

**Received:** 8 February 2025; **Revised:** 22 April 2025; **Accepted:** 14 May 2025

**Graphical Abstract:**

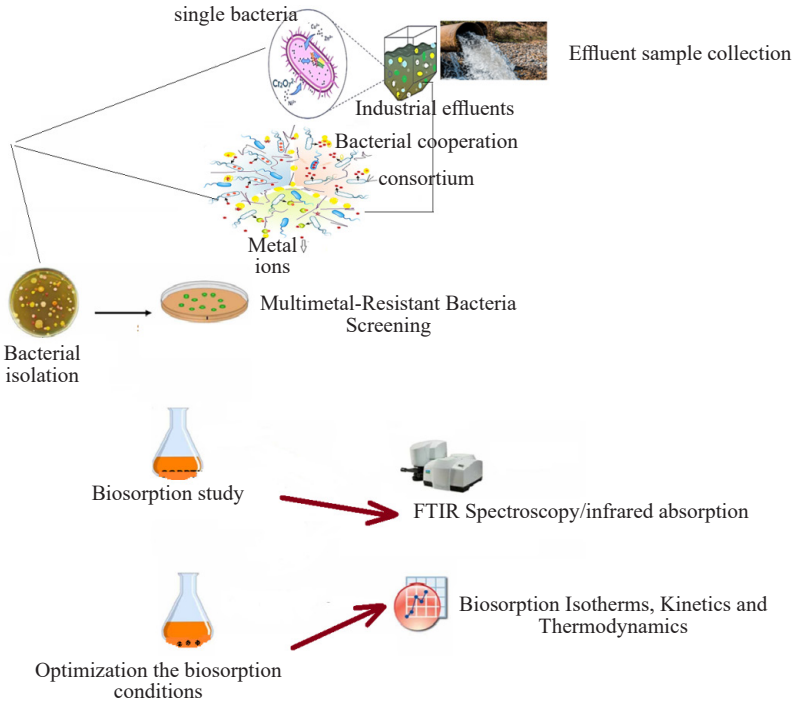


**Abstract:** This study examined the competitive biosorption of metals in single- and multicomponent solutions and the factors influencing metal removal, such as pH, contact time, biosorbent dosage, and initial metal concentration. It evaluated the properties of co-biosorption and the applicability of copper (Cu), zinc (Zn), nickel (Ni), and chromium (Cr) metal ions from aqueous solutions onto biomass from electroplating effluents under ideal conditions. The study


DOI: https://doi.org/10.37256/fce.6220256530

used a single isolate of *Kocuria rhizophila* and a consortium of three isolates: *Bacillus megaterium*, *Sphingobacterium ginsenosidimutans*, and *Kocuria rhizophila*. Isotherms, kinetics, and thermodynamics were used to analyse experimental data. The findings showed that, at a pH of 6.0 and a biomass dosage of 1.5% (0.9 g/L), the consortium achieved better biosorption conditions than the single biomass. It had values of 33.11 mg/g for Ni and 28.81 mg/g for Cr, while the values were 26.88 mg/g for Ni and 21.65 mg/g for Zn at pH 5.0 and a biomass dose of 2.0% (0.898 g/L) for *K. rhizophila*. These values were obtained at the same contact time of 50 minutes and a temperature of 37 °C. The Langmuir model accurately predicted the equilibrium data for metals, outperforming other models except for copper with the consortium, which better complied with the Freundlich model. It was also found that the experimental results and the pseudo-second-order kinetic model largely agreed, except for the quaternary system using the consortium, which complied better with the pseudo-first-order model. The results revealed that the biosorption process was spontaneous and endothermic in nature. The biomass consortium of *B. megaterium*, *S. ginsenosidimutans*, and *K. rhizophila* could effectively remove mineral mixtures from electroplating effluent under optimized conditions for bioprocessing electroplating effluents with weak acidity or close to neutral pH at a medium temperature.

***Keywords*:** equilibrium isotherms, kinetic models, thermodynamics, multicomponent solution, consortium, bacterial isolates, single-component solution

## Nomenclature

| | |
|---|---|
| 16S rRNA | 16S ribosomal RNA, is the RNA component of the 30S subunit of a bacteria ribosome |
| $C_f$ (or $C_e$) | The final or equilibrium concentration of metal (mg/L) |
| $C_i$ | Boundary layer thickness in the Intraparticle diffusion model |
| $C_0$ | The initial concentration of metal in the solution (mg/L) |
| Cr | Chromium element |
| Cu | Copper element |
| $E$ | The free energy of biosorption per adsorbate molecule (kJ/mol) |
| $E_c$ | Electrical conductivity |
| $\varepsilon$ | The Polanyi potential (J/mol) |
| $h$ | The initial sorption rate |
| $HNO_3$ | Nitric acid |
| $H_2O_2$ | Hydrogen peroxide |
| ICP-MS | Inductively Coupled Plasma Mass Spectrometry |
| $K_1$ | The first-order reaction rate constant ($min^{-1}$) |
| $K_2$ | The equilibrium constant of pseudo-second order adsorption (g/mg min) |
| $K_f$ | Freundlich isotherm constant (mg/g) |
| $K_L$ | The Langmuir biosoption constant (L/mg) related to the free energy of biosorption |
| $K_T$ | The equilibrium binding constant (L/g) |
| $k_{int}$ | The intraparticle diffusion rate constant (mg/g $min^{-1/2}$) |
| $K_{eq}$ | The thermodynamic equilibrium constant |
| $n$ | Adsorption intensity |
| Ni | Nickel element |
| OD | Optical Density-a spectrophotometric unit used to quantify bacterial cells |
| OD600 | Optical Density at wavelength 600 nanometer of cells |
| pH | A numerical measure of the acidity or alkalinity of a solution |
| Zn | Zinc element |
| $Q$ | Metal removal rate |
| $q$ | The amount of metal absorbed (mg/g) |
| $q_e$ | The amount of metal ion adsorbed (mg/g) at equilibrium |
| $Q_{max}$ | The maximum monolayer biosoption capacity of the biosorbent (mg/g) |

| | |
|---|---|
| $Q_S$ | The equilibrium theoretical saturation capacity (mg/g) |
| $q_t$ | The amount of metal ion adsorbed (mg/g) at time, $t$ (min) |
| rpm | Revolutions Per Minute |
| $R$ | The universal gas constant (8.314 J/mol/K) |
| $R_L$ | Hall isolation factor. The affinity of the adsorbent to the adsorbate |
| $T$ (K) | The absolute temperature at 298 K |
| $t^{1/2}$ | The square root of time |
| $V$ (L) | The metal solution volume |
| $W$ (g) | The amount of biosorbent or the used biomass |
| $\alpha$ | The Elovich constant (mg/g·min) |
| $\beta$ | The Dubinin-Radushkevich isotherm constant related to biosorption energy per mole of the adsorbate ($mol^2/kJ^2$) |
| $\beta$ | The Elovich constant (g/mg) |
| $\Delta G°$ | Gibbs free energy change |
| $\Delta H°$ | The change in enthalpy is the measurement of energy in a thermodynamic system |
| $\Delta S°$ | The change in entropy the extent to which energy is dispersed throughout a system |

# 1. Introduction

Environmental pollution of heavy metals is a major problem, most notably in electroplating industries that mostly produce effluents containing heavy metals.[1,2] These metals include zinc (Zn), nickel (Ni), cadmium (Cd), chromium (Cr), lead (Pb), copper (Cu), arsenic (As), and others, which are difficult to decay naturally in the environment and are found in high concentrations in industrial electroplating effluent.[3] The removal of toxic heavy metals from water bodies is an absolute necessity to prevent and reduce pollution from being transported further into the environment. Biosorption is one of the most effective methods to remove toxic compounds from polluted sites.[4]

Biosorption research primarily focuses on single-metal solutions, which do not accurately reflect polluted environments with multiple metals. While the sorption mechanisms of individual metals are well understood, competitive interactions between multiple metal ions during the biosorption process are less studied.[5] Despite the complexity of pollutants in industrial and municipal effluents, fewer studies have investigated the competitive or simultaneous removal of metals from multi-metal systems.[6] Further research is needed to manage complex solutions and unstable biomass situations. Further applied research is required to validate laboratory results and promote biosorption as a competitive wastewater treatment technique.[7] As single-metal synthetic solutions for metal adsorption research are outdated, requiring adaptation to wastewater complexity. That is because the behaviour of biosorbents with competing sorbates with different physicochemical properties is not taken into account in the majority of biosorption research employing single or bimetallic solutions. Multi-component systems improve the representation of actual wastewater, focusing on metal competition.[8] However, multimetal systems often have modelling limitations, necessitating more complex models due to the inability of single-metal data-based biosorption models to accurately predict their behaviour.[9] A study comparing biosorption efficiency between single and multi-metal solutions found reduced efficiency due to the competitive effect between metal ions in mixed metal ions, highlighting the need for further research on such systems.[10]

Biosorption research has seen a significant increase in the past 30 years, particularly in heavy metal recovery.[7] The use of microbes for this process is increasingly popular due to their security, efficiency, cost-effectiveness, and high metal recovery. This technique offers minimal secondary pollutant accumulation, cost-effectiveness, and high metal recovery, making it a potentially exploitable technique.[11,12] Microorganisms like bacteria, mould, yeast, and algae can tolerate and accumulate heavy metals, which can be converted into biomass and energy. This method treats wastewater-using bacteria as biosorbents, which eventually aids in restoring the environment and preventing further pollution.[13] It was reported that the greatest research has been done on the biosorption of heavy metals utilizing bacteria;[7] due to their diversity in the natural environment, they are valuable sources for bioremediation of many contaminants. Numerous materials (living or dead biomass) are available for ongoing research to determine the effectiveness of heavy metal bioremediation.[14] It also was stated that both fungus and bacteria are efficient producers as biosorbents that can reduce

heavy metal ion concentrations in solution and sequester metals.[15] The efficiency of biosorption is determined by the composition of the cell wall and metal-binding functional groups. Microorganisms eliminate heavy metals via surface adsorption, which occurs in various physiochemical conditions, including temperature, pH, and ion presence.[16] Their quick kinetics allow them to handle large wastewater quantities.[17]

Heavy metal pollution occurs predominately as a mixture of various pollutants. Thus, bacteria in contaminated sites are usually exposed to a mixture of metals, not individual metals. It is mainly important to consider bacteria capable of treating these contaminants as combined mixtures as well as individual metal solutions. This can lead to a synergistic or antagonistic effect on the treatment of the synthesized combined mixtures, depending on their interactions with each other as well as with the bacteria.[18] It was found that the cells capable of accumulating heavy metals might tolerate one or more metals at higher concentrations.[19] That is because toxic metal ions are detoxified or converted into non-toxic, stable, and inert forms.[20] Therefore, examination of these interactions can determine the bacterial efficiency to grow and tolerate the composite mixtures of metals.

In multimetal biosorption, metal bioremoval is influenced by the metals and the combination of their concentrations in the multimetal solution. Furthermore, the presence of one of the metals in the multimetal solution can have a strong negative effect on the bioremoval of all other metals, due to the strong metal interaction with the functional groups present on the biomass as well as the small radius of this metal in solution (the smaller the radius, the higher its binding affinity).[21,22] Given the limited number of active sites on the biosorbent surface, it is accepted that the biosorption capacity of the biosorbent towards a specific pollutant (metal or nonmetal) in a multicomponent solution is inferior to that in a single-component solution; thus, contaminants will compete for the active sites available for sorption. The electronegativity and atomic weight of metals in multi-metal solutions can also play a crucial role in the biosorption process and efficiency.[22]

Furthermore, it is critical to understand the types of interacting effects among the heavy metals in order to optimize the competitive and simultaneous removal of more than one heavy metal ion in the presence of other cations and anions in multi-solute systems. Competitive sorption often occurs in multicomponent systems, and three types of effects are possible: synergism, antagonism, and non-interaction.[23] To determine the interaction among the components, the adsorption capacity of a pollutant in a solution containing only that single component ($q_{i,\,s}$) and the capacity in a multicomponent solution ($q_{i,\,m}$) should be considered. Individual component adsorption capacity is lower than capacity when present in a multicomponent solution, i.e., $q_{i,\,m} > q_{i,\,s}$ and this is known as synergic interaction. The adsorption of the adsorbate in individual solutions is greater than that of the component in multicomponent solutions, i.e., $q_{i,\,m} < q_{i,\,s}$ and this is referred to as antagonistic interaction. The presence or absence of additional pollutants in the solution has no influence on pollutant adsorption, i.e., $q_{i,\,m} = q_{i,\,s}$ and this is known as non-interaction as clarified.[24,25]

The co-biosorption study of metals in aqueous solutions can be applied individually and quaternarily to single or consortiums of bacteria with optimum biosorption parameters such as pH, biomass dosage, contact time, and temperature because the biosorption of metals depends on these parameters.[26,27] Factors such as pH, temperature, contact time, shaking speed, and the initial concentration of the pollutant or amount of biosorbent will affect the efficacy of the bioprocessing; thus, they should be determined and evaluated to optimize the biosorption process, as reported previously.[28] In addition, adsorbent features such as surface charge, structure, size, porosity, number of active sites, and functional groups present on the sorbent surface may influence the adsorptive removal of one pollutant in a multicomponent system.[24,29] In a multicomponent system, the amount of pollutant removed by the sorbent material may increase, decrease, or remain steady in the presence of other pollutants.[30]

In general, the effects of the simultaneous presence of multiple chemicals have not received as much attention as the effects of single metals. The effects of multiple chemicals are more dangerous than single effects and should not be neglected.[31] There is not enough data for combined toxicological interactions for heavy metals, and there is not much literature indicating the interactions of heavy metals with each other as well as with the biosorbent in the composite mixtures.[32]

Even though research on biosorption processes has been well documented in the literature, biosorption of different metal ions by various types of biological materials has primarily been undertaken in single-metal solutions.[32] Biosorption experiments in binary,[33] tertiary,[34] and quaternary-component solutions are quite rare. Over the last few decades, there has been a great deal of study and research on biosorption techniques for treating contaminated environments and wastewater. However, it is questionable whether such a substantial increase in published output has

meaningfully improved understanding of the biosorption process or supported any industrial exploitation, which is frequently the major underlying concept for such investment and study.[35,36]

This study compares the metal uptake efficiency of individual bacterial isolates with a consortium designed for single and mixed metal solutions. It evaluates whether the consortium has synergistic benefits or antagonistic effects compared to individual strains. The study also explores the nutritional effects of metals like zinc, nickel, and copper, which are essential for bacterial metabolism, compared to nonessential ones like chromium. It investigates whether their co-presence results in competition for uptake sites or if they have synergistic effects at low concentrations and antagonistic effects at higher concentrations. It also examines sequential adsorption, determining whether bacteria preferentially adsorb certain metals over others in a mixture and analyses whether metals compete for the same binding sites on bacterial cell surfaces or if different mechanisms exist for each metal using equilibrium isotherm studies. This research incorporates novel research methods using living cells and explores their potential for cost-effective and environmentally sustainable bioremediation in settings with multiple metal components.

For those purposes, a full comparison was performed to demonstrate the efficiency of a single bacterium, *K. rhizophila*, and a consortium of living biomasses of three isolates, *B. megaterium*, *S. gensenosidmutans*, and *K. rhizophila*, in the removal of Cu, Zn, Ni, and Cr as individual and quaternary metals from liquid effluents. That is for cost-effective and environmentally sustainable bioremediation of contaminated sites. Different parameters influencing the biosorption process were evaluated. To elucidate the possible interaction mechanisms, the biosorbents were characterized based on equilibrium isotherms, kinetic mechanisms of biosorption, and the biosorption thermodynamics for individual and quaternary metals. This study contributes to the experimental testing of multi-metal systems compared to single-metal systems since it reflects real effluent. Multimetal removal is also the most affordable option. Since a variety of mathematical models have been developed for single metal removal, it is critical to focus on multiple metals to comprehend modelling techniques capable of describing living biomass adsorbents in multiple metal systems.

## 2. Material and methods

### 2.1 *Wastewater sample collection*

The direct and ultimate effluent outlets of Yew Hup Metal Electroplating Works, situated at 1 and 2 Jalan Tameng 10, Tameng Jaya Industrial Park, 43300 Seri Kembangan, Selangor, Malaysia, were the source of the electroplating wastewater samples. Large-scale electroplating operations for metals such as copper, cobalt, nickel, nickel-chromium, black, trivalent, blue, and tin-nickel are the plant's area of expertise. Three samples—one near the outlet, one in the center of the effluent stream, and the last one at the end of the effluent outlet—represent various locations inside the site. Between Latitude 3° 0153.1″ N and Longitude 101° 4140.5″ E is where the metal electroplating plant's direct and ultimate outlets are situated. The obtained samples were stored at 4 °C on ice before being brought into the lab to avoid contamination and extend their shelf life.[37]

### 2.2 *Heavy metal solution preparation*

Zinc sulfate ($ZnSO_4$), copper sulphate ($CuSO_4$), potassium chromate ($K_2Cr_2O_7$) (R&M Chemical), and nickel chloride ($NiCl_2$) (HmbG Chemical) were dissolved in double-distilled water to provide stock solutions with 1,000 mg/L concentrations of Zn, Cu, Cr, and Ni. To achieve total dissolution, the solutions were then agitated for 15 minutes and then allowed to stand for 24 hours. A membrane filter was used to sterilise the metal solutions, which were then kept at 4 °C.[38]

### 2.3 *Identification and isolation of bacterial strains resistant to metals from the electroplating effluent*

According to Alhammadi et al.,[39] the bacteria were isolated from collected samples by serial dilution in sterilized phosphate buffer saline solution. The samples were spread on nutrient agar plates supplemented with heavy metals individually and quaternary heavy metals Cr, Zn, Cu, and Ni in the form of their salts, $K_2Cr_2O_7$, $ZnSO_4$, $CuSO_4$, and $NiCl_2$ at concentrations ranging from 10 to 50 mg/L, respectively. To achieve pure cultures at the same concentration of heavy metals, the bacteria were further subcultured. Abbreviations BMA-1, ACM-2, DMA-3, STM-4, BSM-5, BME-6,

A6MA-7, MIC-8, and RMA-9 were assigned to the isolates, which were then kept for further use at 4 °C.

### 2.3.1 *Characterization and diagnosis of bacterial isolates*

The purified isolate was subjected to identification, which included morphological and cultural characterization and biochemical characterization according to Bergey's Manual of Systematic Bacteriology,[40] and finally at the molecular level using rRNA sequencing. The sequencing of 16S rRNA determined the molecular identification or genotype of the isolates from the nutrient agar.[41]

The genomic DNA was extracted and amplified from purified bacterial isolates using an extraction kit (Rapid bacterial genomic DNA isolation kit, Biobasic Inc.), according to the manufacturer's protocol. 16s rRNA genes with a full length of 1.5 kb were amplified using universal primer 27-F 5' (AGA GTT TGA TCM TGG CTC AG) '3 and reverse primer 1492-R 5' (TACGGY TAC CTT GTT ACG ACT T) 3'. The PCR mixture of 25 µL consisted of 10.5 µL nuclease free water, 12.5 µL OneTaq. 2X Master Mix (NEB), 0.5 µL, 10 µM of each 27-Fand 1492-R with 1 µL of 50 ng DNA as templates. According to the protocol at Bio3 Scientific SdnBhd, Puchong, Selangor, Malaysia, PCR was performed at 94 °C for 4 min to initiate denaturation, followed by 30 cycles of denaturation at 94 °C for 30 s, annealing at 55 °C for 30 seconds, and extension at 68 °C for 1 min and 30 seconds and final extension at 68 °C for 5 minutes. Following the annealing and extension of the amplified DNA, 1% (W/V) agarose gel electrophoresis, a common technique for most applications, was used to purify the products of PCR. Sequencing was performed by the BioBasic sequencing facility. Sequencing results were analyzed using the Sequence Scanner V1.0 (Applied Biosystem), edited and assembled using Chromas. The assembled sequence was then subjected to a homology search in the National Center for Biotechnology Information (NCBI) nucleotide collection 16s database excluding uncultured/environmental sample sequences using Basic Local Alignment Search Tool (BLAST). The top ten BLAST results were used to construct an unrooted neighbor-joining phylogenetic tree using BLAST Software.

After the bacterial isolates were prepared, their growth, resistance, and biosorption capacities were evaluated. Based on which isolates showed the greatest degree of metal resistance, three isolates were selected.

## 2.4 *Heavy metal minimum inhibitory concentration calculation*

Heavy metals' Minimum Inhibitory Concentration (MIC) was calculated in accordance with Alhammadi et al.[39] The isolates were inoculated with 100-500 mg/L of each metal, both individually and quaternarily, in 50 mL of sterile nutrient broth. After that, the incubation was conducted for 24 hours at 37 °C and 150 rpm, and an Atomic Absorption Spectrophotometer (AAS) was used to measure the growth at 600 nm. The bacteria were inoculated into a metal-deficient medium, which served as a positive control. According to a previous report,[42] isolates with a value greater than 0.1 were deemed to have positive growth and resistance. After sterilizing the medium with filtering from filter-sterilized stock solutions, all metal salts were added.[43] After achieving growth, each isolate was moved on to the following concentration. The variation in the experimental data regarding the minimum inhibitory concentration of bacteria resistant to metals was expressed as the Standard Deviation (SD).

## 2.5 *Bacterial isolate growth and tolerance to heavy metals*

Sterile Zn, Cu, Cr, and Ni heavy metals at the highest initial concentrations (100 mg/L) were added to a nutrient broth, then overnight isolates with an OD = 0.6 were inoculated into the nutrient broth that contained heavy metals. The metals were added individually and quaternarily in a 250 mL Erlenmeyer flask to each culture medium flask. The flasks were then incubated for 24 hours at 37 °C. The optical density at 600 nm with a metal-free bacterial culture was used to measure the isolates level of tolerance.

### 2.5.1 *Biosorbent characteristics*

Using PerkinElmer's Fourier Transform Infrared (FTIR) spectroscopy, the functional groups in the biosorbent were identified. The infrared spectra were captured in the 400-4,000 $cm^{-1}$ range.[39]

### 2.5.2 *FTIR spectroscopy analysis*

The strongest metal-tolerant overnight bacterial cultures were supplemented with 100 mg/L of individual and quaternary metals, the unaltered cultures were centrifuged for five minutes at 10,000 rpm, and the pellets were lyophilized. 2 mg of the bacterial pellets were combined with 200 mg of KBr powder to create sample discs, which were then subjected to FTIR analysis. A qualitative and initial characterization of the main functional chemical groups present in living biomass and in charge of heavy metal biosorption was provided by Fourier Transform Infrared (FTIR) spectroscopy spectra. On a Perkin Elmer (FT-IR) spectral (Perkin Elmer Spectrum 100 FTIR, Waltham, MA, USA), functional groups that were in charge of metal absorption in the metal-laden and unladen bacteria (*B. megaterium*, *S. ginsenosidimutans*, and *K. rhizophila*) were examined in the 400-4,000 $cm^{-1}$ range.[39]

## 2.6 *Co-biosorption from aqueous solution of metal ions, isotherms, kinetics and thermodynamics of biosorption*

Each batch experiment was performed in 100-mL Erlenmeyer flasks with individual metals (Cu, Zn, Ni, and Cr) and quaternary. The term "quaternary" refers to the mixture of four previous metals. Batch experiments were studied at various parameters, including pH, inoculation dosage, metal concentrations, temperature, and contact time. The biosorption characteristics of individual metals and quaternary from aqueous solution using a single isolate, *K. rhizophila* and consortium of three isolates, *B. megaterium*, *S. ginsenosidimutans* and *K. rhizophila*, were investigated using Inductively Coupled Plasma Mass Spectrometry (ICP-MS).

### 2.6.1 *Effect of pH*

100 mL of nutrient broth medium was used to cultivate aliquots of 1,000 suspensions of one isolate of *K. rhizophila* and a consortium of three isolates (*K. rhizophila*, *B. megaterium*, and *S. ginsenosidimutans*) that were 24 hours old and had an OD of 0.6. They were then incubated for 24 hours at 37 °C and 150 rpm in an agitated circumstance. For 20 minutes, the cultures were centrifuged at 4,000 rpm. After discarding the supernatant, the bacterial pellet was subjected to cell washing with sterile saline water and dilution until the Optical Density (OD) reached 0.6 (at 600 nm). In a 250 mL Erlenmeyer flask, an aliquot of 1% suspension of the isolate bacterial suspension (24 hours old) with OD = 0.6 was inoculated in 100 mL of nutrient broth medium that was pH-adjusted at 5, 6, 7, 8, and 9 and contained 100 mg/L concentrations of $Zn^{2+}$, $Cu^{2+}$, $Cr^{2+,}$ and $Ni^{2+}$ as primary and quaternary solutions.[44-46] Erlenmeyer flasks were incubated for 24 hours at 150 rpm and 37 °C. Following the drawn 5 mL samples, they were centrifuged for 20 minutes at 4,000 rpm. The ideal pH was determined by repeating each experiment with a different pH. After collecting the supernatants, they were digested using a double volume of each of $HNO_3$ (67% v/v) and $H_2O_2$ (30% v/v). To finish acid digestion, the mixtures were heated to 100 °C on a hot-plate stirrer until the final volume was lowered to the volume of the original supernatant. The extracts were then collected into a volumetric flask, diluted, and filtered through filter paper (Whatman 42) to eliminate any remaining insoluble material. The equilibrium uptake capacity and the amount of metal ion that were adsorbed were computed for each sample using Inductively Coupled Plasma Mass Spectrometry (ICP-MS).

### 2.6.2 *Effect of inoculation dose*

The three isolates (*K. rhizophila*, *B. megaterium*, and *S. ginsenosidimutans*), with a single isolate of *K. rhizophila*, were cultivated in 100 mL of nutrient broth medium (at the ideal pH for each metal) and incubated under agitated conditions for 24 hours at 150 rpm and 37 °C. For 20 minutes, the cultures were centrifuged at 4,000 rpm. Following the disposal of the supernatant, the bacterial pellet was subjected to cell washing with sterile saline water and dilution until the Optical Density (OD) reached 0.6 (at 600 nm). As reported by Jaafar et al.,[44-46] aliquots of 0.1%, 0.5%, 1.0%, 2.0%, and 3.0% of the total medium volume of the bacterial cultures (24 hours old) with OD = 0.6 were inoculated in a 250 mL Erlenmeyer flask with 100 mg/L concentrations of $Zn^{2+}$, $Cu^{2+}$, $Cr^{2+}$, and $Ni^{2+}$ as individual and quaternary solutions. For 24 hours, the Erlenmeyer flasks were incubated at 37 °C and 150 rpm. A total of five milliliter samples were collected and centrifuged for 20 minutes at 4,000 rpm. After collecting the supernatants, they were digested in a double

volume of each of $HNO_3$ (67% v/v) and $H_2O_2$ (30% v/v). To achieve acid digestion, the mixtures were heated to 100 °C on a hot-plate stirrer until the final volume dropped to the volume of the original supernatant. The extracts were then filtered through filter paper (Whatman 42), collected into a volumetric flask, and diluted in order to finish acid digestion, lower the final volume to the initial supernatant volume, and eliminate any insoluble material. Inductively Coupled Plasma Mass Spectrometry (ICP-MS) was used to analyze the equilibrium uptake capacity and the quantity of metal ions adsorbed for each extract. Other factors were investigated using the inoculation doses from the single bacteria and consortium that produced the highest biosorption. To determine the dry weight (gm) of the biomass used, the amount of biomass generated with each type of metal was also dried and weighed.

### 2.6.3 *Effect of metal concentration*

As reported by Jaafar et al.,[44-46] different initial metal concentrations (10, 50, 100, 150, and 200 mg/L) of $Zn^{2+}$, $Cu^{2+}$, $Cr^{2+}$, and $Ni^{2+}$ as individual and quaternary solutions in 250 mL Erlenmeyer flasks were used to cultivate a single isolate of *K. rhizophila* and a consortium of three isolates (*K. rhizophila*, *B. megaterium*, and *S. ginsenosidimutans*) in 100 mL of nutrient broth medium (at the optimal pH with each metal and biomass dosage). The Erlenmeyer flasks were incubated for 24 hours at 150 rpm and 37 °C. Following the drawing of 5 mL samples, they were centrifuged for 20 min at 4,000 rpm. The supernatants were gathered and digested using a double volume of each of $HNO_3$ (67% v/v) and $H_2O_2$ (30% v/v). To finish acid digestion, the mixtures were heated to 100 °C on a hotplate stirrer until the final volume was lowered to the volume of the original supernatant. The extracts were then collected in a volumetric flask, diluted, and filtered through filter paper (Whatman 42) to eliminate any insoluble material. ICP-MS was used to analyze the equilibrium uptake capacity and the quantity of metal ions adsorbed for each extract.

### 2.6.4 *Effect of temperature*

A consortium of three isolates (*K. rhizophila*, *B. megaterium*, and *S. ginsenosidimutans*) and a single isolate of *K. rhizophila* were cultivated in 100 mL of nutrient broth medium (at the ideal pH for each metal, biomass dosage, and metal concentration) and incubated at various temperatures (20, 25, 37, 42, and 50 °C) under agitated conditions at 150 rpm for 24 hours. Five milliliters of samples were collected and centrifuged for 20 minutes at 4,000 rpm. The supernatants were gathered and digested using a double volume of them, $HNO_3$ (67%), and $H_2O_2$ (30% v/v). The mixtures were heated to 100 °C on a hot-plate stirrer to finish the acid digestion process, reducing the final volume to the volume of the original supernatant. The extracts were then filtered through filter paper (Whatman 42) to eliminate any insoluble material, gathered into a volumetric flask, and diluted. Using ICP-MS, the extracts' residual metal concentrations were examined. In each solution, the equilibrium uptake capacity and the concentration of residual metal ions were measured.[44]

### 2.6.5 *Effect of equilibrium time*

Three isolates (*K. rhizophila*, *B. megaterium*, and *S. ginsenosidimutans*) and a single isolate of *K. rhizophila* were cultivated in 100 milliliters of nutrient broth medium (at the optimal pH with each metal, biomass dosage, metal concentrations, and temperature). The Erlenmeyer flasks were incubated at 150 rpm for varying periods (10, 20, 30, 40, 50, 60, and 70 minutes) in an agitated circumstance. Five-milliliter samples were collected and centrifuged for 20 minutes at 4,000 rpm. In a double volume, the supernatants were gathered and digested using $HNO_3$ (67% v/v) and $H_2O_2$ (30% v/v). To finish acid digestion, the mixtures were heated to 100 °C on a hotplate stirrer until the final volume was lowered to the volume of the original supernatant. The extracts were then filtered through filter paper (Whatman 42) to eliminate any insoluble material, gathered into a volumetric flask, and diluted. Using ICP-MS, the extracts' residual metal concentrations were examined. For each extract, the amount of metal ions adsorbed and the equilibrium uptake capacity were determined.[44]

## 2.7 *Modelling and calculation of metal biosorption in single and multicomponent system*

Inductively coupled plasma mass spectrometry was used to determine the residual metal concentrations in the extracts and across all tests. All the experiments were carried out in triplicate, and the results were calculated by

equation (1), which represents the percentage biosorption of heavy metal by isolates in single and multi-component systems.[47]

$$Q = \frac{C_0 - C_e}{C_0} \times 100\% \quad (1)$$

Where: $Q$ is the metal removal rate, $C_0$ is the initial concentration of metal in the solution (mg/L), and $C_e$ is the final concentration of metal in the solution (mg/L). Then, the amount of metal ions adsorbed per gram of biomass and metal uptake at equilibrium were calculated using the equation (2):

$$q_e = \frac{(C_0 - C_e) \times V}{W} \quad (2)$$

Where: $q_e$ is the amount of metal absorbed (mg/g), $C_0$ is the initial metal concentration (mg/L), $C_e$ or ($C_f$) is the final or equilibrium concentration of metal (mg/L), $V$ (L) is the metal solution volume, and $W$ (g) is the amount of biosorbent or the used biomass.[48]

To further define the sorption mechanism, the Langmuir, Freundlich, Temkin, and Dubinin-Radushkevich models were used to describe equilibrium adsorption isotherms in single and multi-component systems. Table 1 lists the isotherm models in single systems as well as their equations and constants. In the case of the multicomponent system, isotherms of multicomponent absorption have been developed that combine equilibrium data from a single system with additional information from a multicomponent system, Table 2 shows isothermal models for multicomponent systems.

Furthermore, different kinetic models were also used to clarify the adsorption kinetics of heavy metal ions under optimal operating conditions by single bacteria and consortium. The adsorption kinetics of metal uptake were studied using the pseudo-first-order, pseudo-second-order, Elovich equation, and an intra-particle diffusion model. Table 3 lists the various kinetic models and their constants used in this study.

**Table 1.** The isotherm models in the single-component system employed in this study

| Adsorption isotherms | Equation | Parameters | Plot | Reference |
|---|---|---|---|---|
| Langmuir | $\frac{C_e}{q_e} = \frac{1}{K_L Q_{max}} + \frac{1}{Q_{max}}$ <br> $R_L = \frac{1}{1 + K_{LC_i}}$ | $Q_{max}$, $K_L$, $R_L$ and $R^2$ | $1/C_e$ versus $1/q_e$ from the plot $1/K_L Q_{max}$ and $(1/Q_{max})$ represent the slope and intercept respectively | 49-52 |
| Freundlich | $\ln q_e = \ln K_f + 1/n \ln C_e$ | $n$, $K_f$ and $R^2$ | $\ln q_e$ versus $C_e$ | 51, 53-56 |
| Temkin | $q_e = \beta \ln K_T + \beta \ln C_e$ <br> $\beta = R_T/b$ | $K$, $\beta$, $b$ and $R^2$ | $\ln C_e$ against $q_e$ | - |
| Dubinin-Radushkevich | $\ln q_e = \ln q_s - \beta\varepsilon^2$ <br> $\varepsilon = RT \ln (1 + 1/C_e)$ <br> $E = 1/\sqrt{2\beta}$ | $q_s$, $\beta$, $E$ and $R^2$ | $\ln q_e$ versus $\varepsilon^2$ | 57-59 |

The biosorption process is strongly dependent on the adsorption temperature and the action thermodynamics of the sorption of metal ions onto adsorbents shows whether the sorption process follows physisorption or chemisorption

and describes the difference between them.[60] In physisorption, the adsorbate is attracted to the adsorbent by weak Van der Waals forces and does not require any activation energy. The sorption occurs with increasing temperature, and it is reversible. While chemical bonds can be formed between the surfaces of the adsorbent and the adsorbate in chemisorption, in this case, it is difficult to remove the heavy metals being adsorbed from the adsorbent; therefore, chemisorption is of an irreversible nature.[61] Thermodynamic analysis was performed in the temperature range of 283-313 K to determine thermodynamic constants such as Gibbs free energy change ($\Delta G°$), enthalpy change ($\Delta H°$), and entropy change ($\Delta S°$) for the system and to confirm the adsorption mechanism. The thermodynamic parameters used in this study are given in Table 4.

Variance analysis and data processing of metal biosorption capacity individually and quaternary by single bacteria and consortium at different conditions were conducted using the statistical procedure SPSS 25. The optimal conditions were analyzed using Analysis of variance (ANOVA), and the biosorption rate differences were analyzed using a post hoc Tukey test.

**Table 2.** The isotherm models in the multi-component system employed in this study

| Isotherm model | Isotherm equations | Parameters | Plot | References |
|---|---|---|---|---|
| Langmuir | $q_e = \frac{q_m K_L C_e}{1+\sum_{i=1}^{n} K_{Li} C_{ei}}$ | $K_L$, $q_m$ and $R^2$ | $1/C_e$ versus $1/q_e$ from the plot $1/K_L Q_{max}$ and $(1/Q_{max})$ represent the slope and intercept respectively | 62 |
| Freundlich | $q_e = K_{fi} \sum_{i=1}^{m} C_{ei}^{\frac{1}{n}}$ | $K_f$, $n$ and $R^2$ | $\ln q_e$ versus $C_e$ | 62, 63 |
| Temkin | $q_e = \beta_{1i} \sum_{i=1}^{n} \ln(K_{Ti} C_{ei})$ | $b_{Te}$, $R$, $K_T$ and $R^2$ | $\ln C_e$ against $q_e$ | 64 |
| Dubinin Radushkevitch (DR) | $\ln Q_e = \ln Q_s - (\beta\varepsilon^2)$<br>$\varepsilon = RT\ln[1 + 1/C_e]$ | $\beta$, $\varepsilon$, $q_{max}$ and $R^2$ | $\ln q_e$ versus $\varepsilon^2$ | 65, 66 |

**Table 3.** The kinetics models in the single and multi-component systems employed in this study

| Kinetics models | Formula | Parameters | plot | Reference |
|---|---|---|---|---|
| Pseudo first-order | $\ln(q_e - q_t) = \ln q_e - (K_1 t / 2.303)$ | $K_1$, $q_e$ and $R^2$ | $\ln(q_e - q_t)$ versus $t$ | 67-69 |
| Pseudo second-order | $\frac{t}{q_t} = \frac{1}{K_2 q_e} + \frac{t}{q_e}$<br>$h = K_2 q_e^2$ | $K_2$, $q_e$ and $R^2$ | $\frac{t}{q_t}$ versus $t$ | 69, 70 |
| Elovich | $q_t = \frac{1}{\beta}\ln(\alpha\beta) + \left(\frac{1}{\beta}\right)\ln t$ | $\alpha$, $\beta$ and $R^2$ | $q_t$ versus $\ln t$ | 70, 71 |
| Intraparticle diffusion | $q_t = k\,\mathrm{int}\, t^{1/2} + C_i$ | $k$ int, $C_i$ $R^2$ | $q_t$ versus $t^{1/2}$ | 70, 71 |

**Table 4.** Thermodynamical parameters for metal sorption employed in this study

| Thermodynamic parameters | Formula | The results of parameters values | plot | Reference |
|---|---|---|---|---|
| Gibbs free energy ($\Delta G$) | $\Delta G = -RT \ln K_L$<br>$\ln K = \frac{\Delta S}{R} - \frac{\Delta H}{RT}$<br>$K = Q_e / C_e$ | $\Delta G < 0$ Spontaneous and feasible process<br>$\Delta G > 0$ Energy requirement for sorption process | | 72, 73 |
| Enthalpy ($\Delta H$) | | $\Delta H > 0$ Endpthermic process<br>$\Delta H < 0$ Exothermic process | $\ln K_{eq}$ versus $\frac{1}{T}$ | 73 |
| Entropy($\Delta S$) | $\Delta G = \Delta H - T\Delta S$ | $\Delta S > 0$ Increase in randomness at solid/ solution interface<br>$\Delta S < 0$ Associated mechanism (decreased randomness) | | 60, 61, 74 |

# 3. Results

## 3.1 *Isolation and identification of metal tolerant bacterial strains from the electroplating effluent*

Using the shake flask enrichment media, a total of 60 bacterial isolates were isolated from electroplating industrial effluents and were able to grow on media incorporating individual and quaternary metals at concentrations of 10-50 mg/L. Initially, nine isolates that were able to grow at the highest concentration of 50 mg/L were chosen for further study.

**Table 5.** Morphological characteristics of bacterial isolates

| Isolates | Colony color | Motility | Gram nature and shape | Cell morphology |
|---|---|---|---|---|
| BMA-1 | Cream to yellow | + | Positive, short rods, coryneform rods single, paired and clumps. | Non-spore-forming Undulate, flat and smooth. |
| ACM-2 | White and grey | - | Positive to variable. | Mycelia or rough and crumbly in texture. |
| DMA-3 | Yellow | + | Positive/Cells were small, short and slender rods and occurred singly or in irregular clusters. | Non-spore-forming, translucent, yellow-pigmented, opaque, circular, low-convex, moist, margins and entire. |
| STM-4 | White and yellowish | - | Positive/cocci. | Non-spore-forming, glistening, with entire margins, smooth, opaque, graped in pairs, tetrads and clusters. |
| BMS-5 | White | + | Positive/rods in chains. | Spores-forming, opaque, waxy, circular with jagged edges. |
| BME-6 | Faint yellow | + | Positive/rods in pairs and chains. | Spores-forming, round, Smooth and flat. |
| A6MA-7 | Orange | - | Negative/coccoid to bacillary. | Non-spores-forming, round, smooth, raised, and glistening with entire edges. |
| MIC-8 | Yellow | - | Positive/cocci pairs, tetrads, and irregular clusters. | Non-spores-forming, circular, shiny smooth, convex, entire and small. |
| RMA-9 | Salmon- | - | Negative/coccoid to bacillary. | Non-spores-forming, smooth, circular, raised, and glistening with entire edges. |

### 3.1.1 *Morphological characteristics of bacterial isolates*

The study revealed that rods, coccobacilli, cocci, non-spore-forming, Gram-positive, and negative bacterial isolates were predominant, with only two spore-forming isolates belonging to *Bacillus* spp. The diverse morphology and intercultural differences among isolated bacteria highlight their unique characteristics and taxonomic diversity, indicating their survival ability and utilization in contaminated environments. This fact was supported by Mathivanan et al.,[75] who reported that exposure of bacteria to harmful environmental conditions induces stress responses, necessitating morphological enhancements for bioremediation based on morphological changes and biomolecule production, which enhances the improvement benefits and mitigates environmental challenges.

The description of cell morphology is represented in Table 5.

### 3.1.2 *Biochemical characteristics of bacterial isolates*

The biochemical characteristics of the isolated bacteria are listed in Table 6. The results demonstrated that isolated bacteria showed different metabolic and enzymatic capabilities.

**Table 6.** The biochemical characterization of bacterial isolates

| Isolates test | BMA-1 | ACM-2 | DMA-3 | STM-4 | BMS-5 | BME-6 | A6MA-7 | MIC-8 | RMA-9 |
|---|---|---|---|---|---|---|---|---|---|
| Catalase | + | + | + | + | + | + | + | + | + |
| Citrate | - | - | + | - | - | + | - | - | - |
| Gelatin | - | - | - | - | + | + | - | + | - |
| Starch | - | - | - | - | + | + | + | - | - |
| Indole | - | - | - | - | - | - | - | - | - |
| Methyl red | + | + | + | - | + | + | - | - | - |
| Voges Proskauer | - | - | - | V | - | - | + | + | - |
| Nitrate | + | + | + | V* | + | + | + | + | V* |
| Urease | - | - | - | - | - | - | - | - | - |
| Utilization of: Glucose | + | + | + | + | + | + | + | + | + |
| Lactose | - | - | + | V | - | + | - | - | + |
| Sucrose | + | + | + | + | + | + | + | - | + |

*Variable results (are positive and negative)

### 3.1.3 *Molecular identification of bacterial isolates*

Isolates BMA-1, CMA-2, DMA-3, STM-4, BMS-5, BME-6, A6MA-7, MIC-8, and RMA-9 were subjected to further identification using 16S rRNA technology. This analysis was used to identify isolates down to the species level because it is more informative and accurate.[76] The genomic DNA extraction of nine bacterial isolates was performed using an extraction kit (Rapid bacterial genomic DNA isolation kit, Biobasic inc.), according to the manufacturer protocol. Agarose gel electrophoresis of the bacteria showed 16S rRNA gene amplicons of approximately 1,500 bp presenting a separation pattern of PCR-amplified genomic DNA (as shown in Figure 1). The bacteria belonged to genera *Microbacterium* spp, *Streptomyces* sp, *Staphylococcus* sp, *Bacillus* spp, *Sphingobacterium* spp, and *Kocuria* sp with a variation at the species level. Their query cover and percentage similarity ranged between 98 to 100% as shown in Table

7. The nucleotide sequences of 16S rRNA of nine isolates documented in this study were deposited in (National Center for Biotechnology Information NCBI) nucleotide sequence databases under Accession Numbers. The percentage of maximum similarity and GenBank accession number are shown in Table 7.

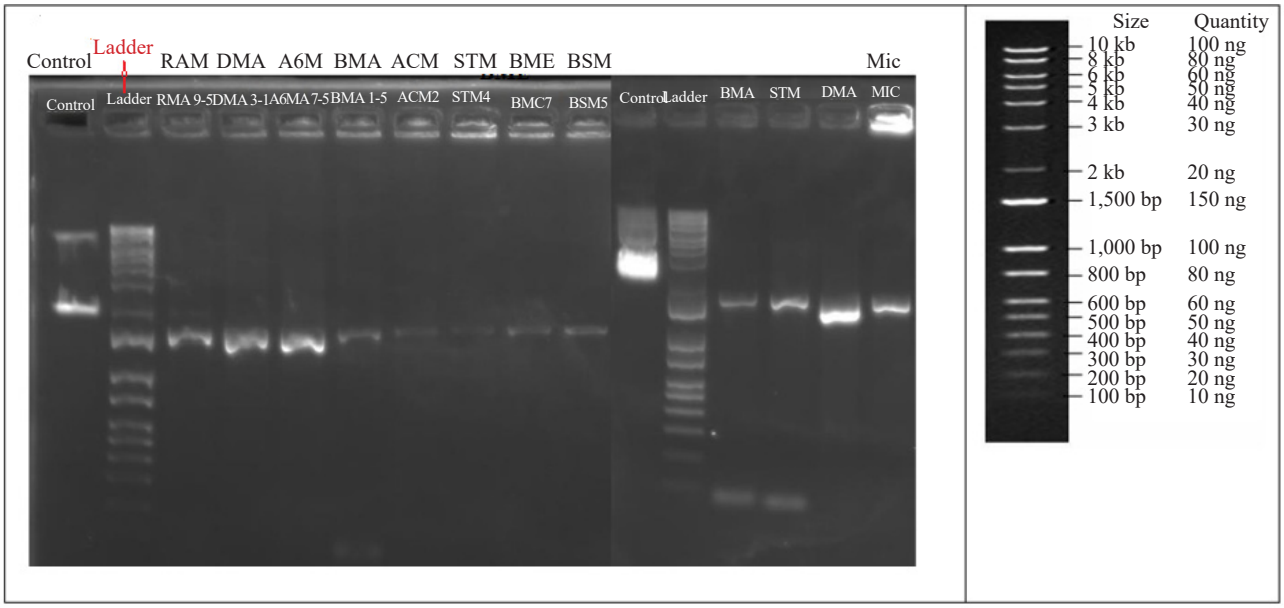


**Figure 1.** Gel electrophoresis of PCR product of the 16S rRNA gene of the bacterial isolates

**Table 7.** BLAST results of the 16SrRNA gene sequences of the isolates at NCBI

| Accession | Description | Query | Query cover % | E. value | Identity % |
|---|---|---|---|---|---|
| NR_025548.1 | *Microbacterium paraoxydans* | BMA-1 | 100 | 0.0 | 99.93 |
| NR_112390 | *Streptomyces werraensis* | ACM-2 | 99 | 0.0 | 99.65 |
| NR_0449321 | *Microbacterium arabinogalactanolyticum* | DMA-3 | 100 | 0.0 | 99.86 |
| NR_036956.1 | *Staphylococcus haemolyticus* | STM-4 | 100 | 0.0 | 99.53 |
| NR_1577341 | *Bacillus paramycoides* | BSM-5 | 99 | 0.0 | 100 |
| NR_117473.1 | *Bacillus megaterium* | BME-6 | 99 | 0.0 | 99.93 |
| NR_108689.1 | *Sphingobacterium ginsenosidimutans* | A6MA-7 | 96 | 0.0 | 98.57 |
| NR_026452.1 | *Kocuria rhizophila* | MIC-8 | 100 | 0.0 | 100 |
| NR_118238 | *Sphingobacterium detergens* | RMA-9 | 100 | 0.0 | 98.01 |

The phylogenetic trees were constructed with the Blast program to illustrate the position of the isolates in the neighbour-joining phylogenetic tree, as shown in Figures 2-9. The isolates were matched with the top comparable group species using a phylogenetic tree and allocated via Genebank submission.

A bacterial phylogenetic tree, built using 16S rRNA gene sequences, is like a family tree showing evolutionary relationships among bacteria. Tips of branches represent different bacteria, including isolates used in this study and

others. Branching points (nodes) indicate a common ancestor; closer nodes mean more recent shared ancestry. Branch lengths often represent the amount of genetic difference in their 16S rRNA gene. Since the 16S rRNA gene is highly conserved but with enough variation, similarities and differences in its sequence help us understand how closely related different bacteria are. Bacteria with very similar 16S rRNA sequences are likely to be more closely related and grouped together on a branch. Bacteria that have a very recent common ancestor (their branches join at a node close to the tips) likely have very similar 16S rRNA sequences and are likely very similar, suggesting they are closely related (different species within the same genus). The branch leading to bacteria joins the main branch much earlier (at a deeper node); its 16S rRNA sequence is more different, indicating that it is more distantly related, possibly from a different genus or even a different family.

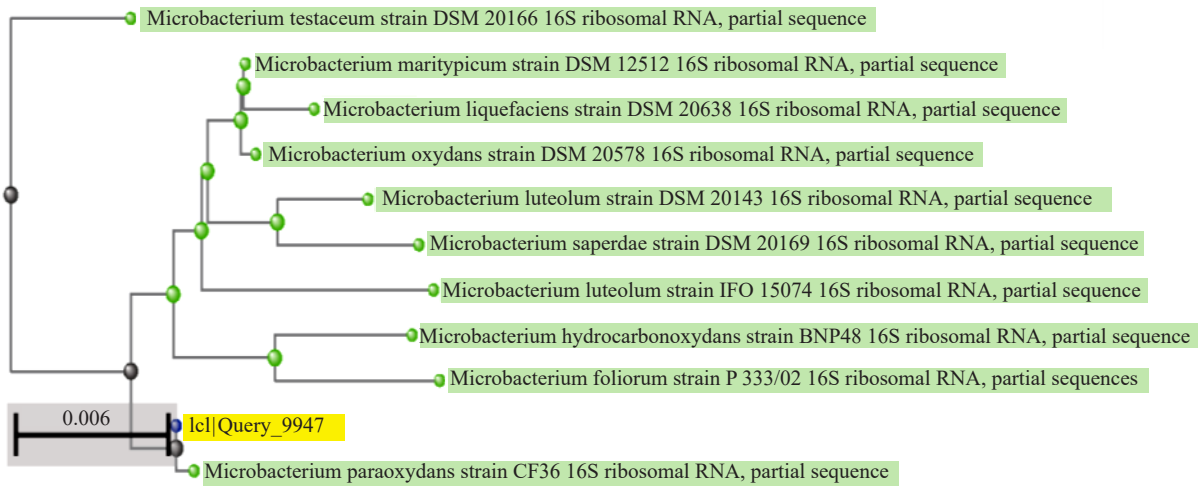


**Figure 2.** Phylogenetic relationship of isolate BMA-1 and closely related sequences based on partial 16S rRNA gene sequence

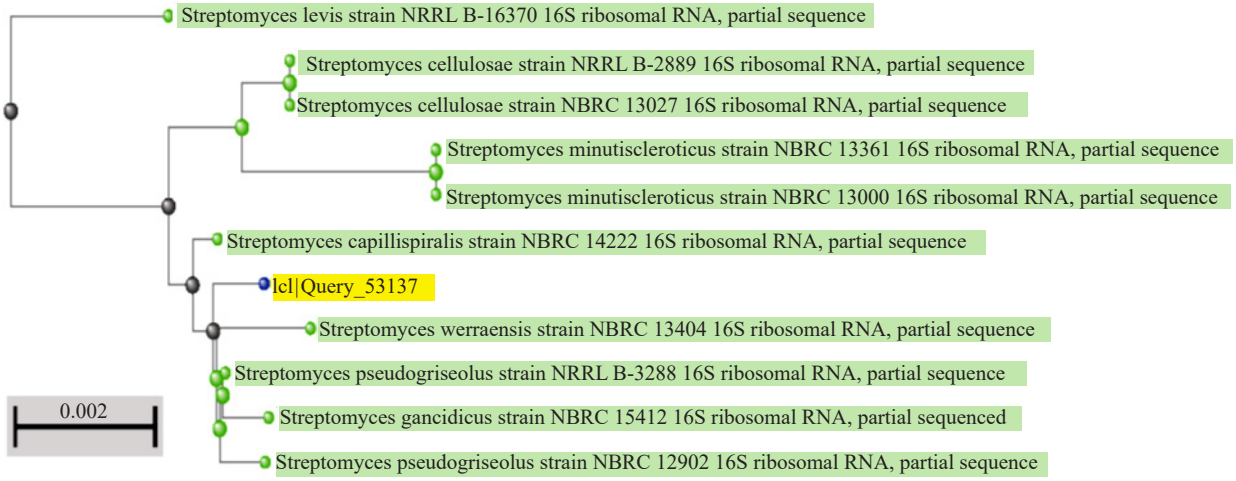


**Figure 3.** Phylogenetic relationship of isolate CMA-2 and closely related sequences based on partial 16S rRNA gene sequence

Schlaberg et al.[77] state that bacteria that have nucleotide base sequence similarity between ≥ 97% and < 99% belong to the same species; bacteria that have a similarity of < 97% are more conservative than new species and are identical to comparative bacterial species; and bacteria that have a similarity of < 95% belong to a new genus. The BLAST results

in Table 7 and Figures 2-9 showed the following:

The BLAST results in Table 7 and Figure 2 show that Isolate BMA-1 has a similarity of 99.93% with *Microbacterium pataoxydans* (NR_025548.1). This shows that the BMA-1 isolate was the same species as *Microbacterium pataoxydans*.

In Table 7 and Figure 3 isolate CMA-2, which had a great similarity with *Streptomyces capillispiralis* (NR_041168.1), but had a closer genetic relationship with *S. werraensis* (NR_112390.1) (99.65%). Thus, it indicates that CMA-2 is the same species as *S. werraensis*.

Isolate DMA-3 had 99.86% similarity with *Microbacterium arabinogalactanolyticum* (NR-044932.1) as illustrated in Table 7 and Figure 4, showing that DMA-3 is the same species as *Microbacterium arabinogalactanolyticum*.

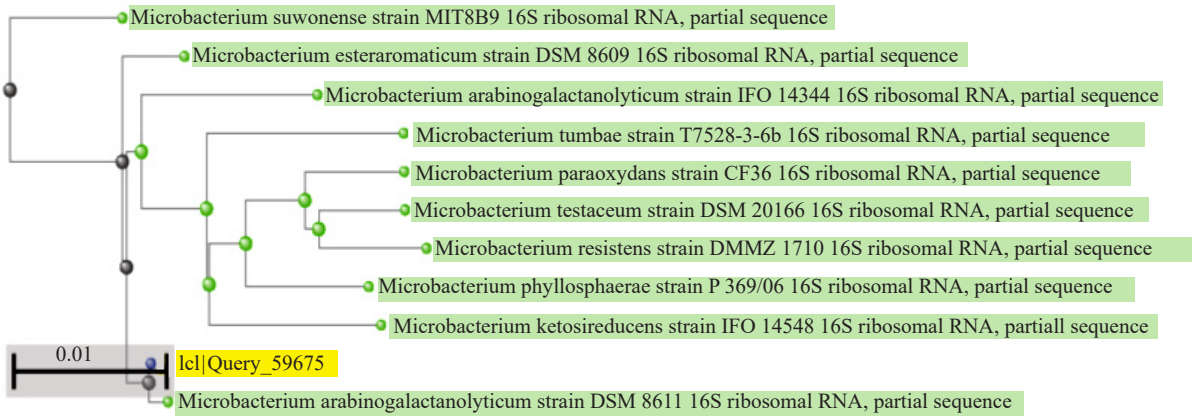


**Figure 4.** Phylogenetic relationship of isolate DMA-3 and closely related sequences based on partial 16S rRNA gene sequence

The STM-4 isolate had a similarity of 99.53% with *Staphylococcus haemolyticus* (NR_036955.1), as stated in Table 7 and Figure 5, showing STM-4 is the same species as *Staphylococcus haemolyticus*.

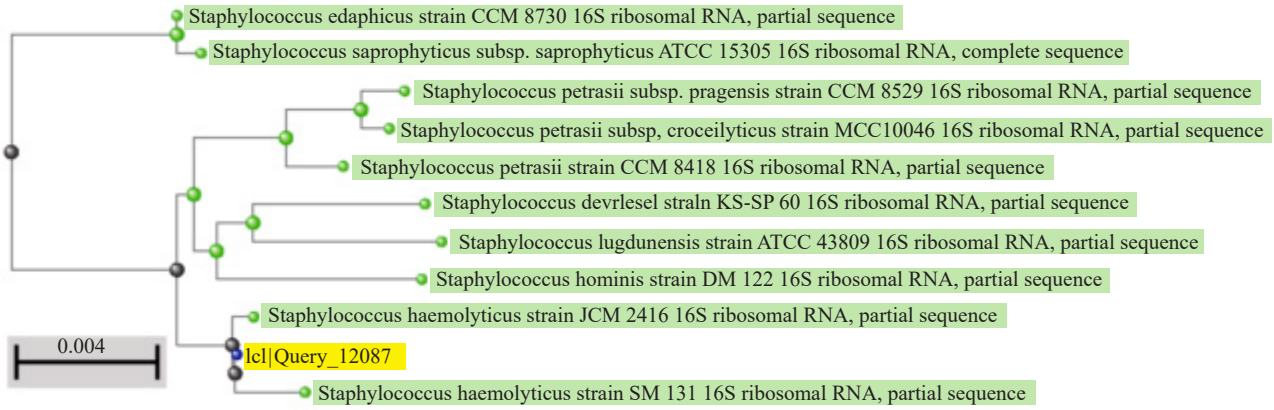


**Figure 5.** Phylogenetic relationship of isolate STM-4 and closely related sequences based on partial 16S rRNA gene sequence

Isolate BSM-5 showed a high similarity ratio of 100% with *Bacillus paramycoides* (NR_157734.1) in Table 7 and Figure 6. Thus, it is the same species as *Bacillus paramycoides*.

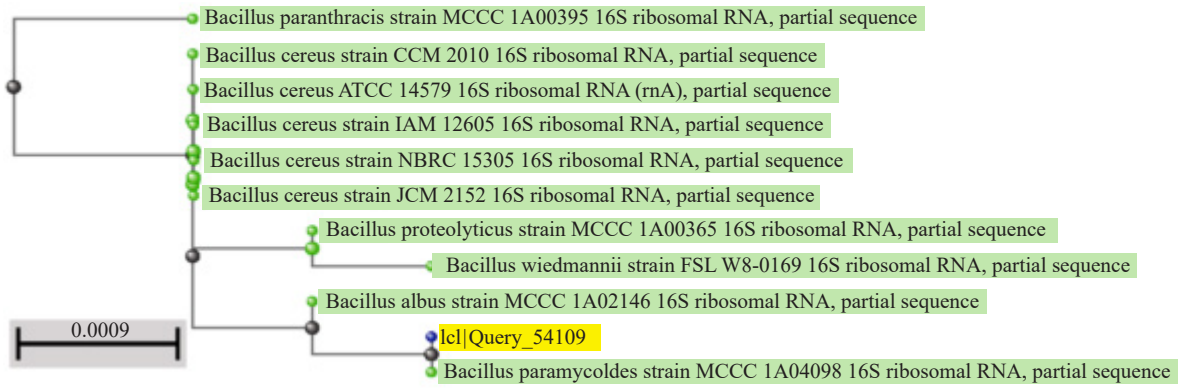


**Figure 6.** Phylogenetic relationship of isolate BSM-5 and closely related sequences based on partial 16S rRNA gene sequence

Isolate BME-6 had a similarity of 99.93% and was the nearest to Bacillus megaterium (NR_117473), as shown in Table 7 and Figure 7. Two previous isolates and the taxonomy were matched with these bacteria due to their showing the closest distance on the phylogenetic tree.

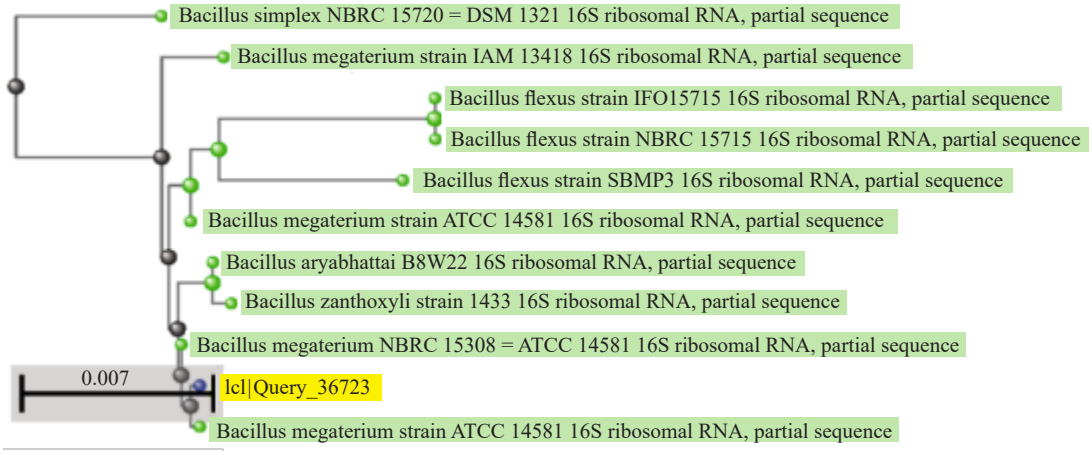


**Figure 7.** Phylogenetic relationship of isolate BME-6 and closely related sequences based on partial 16S rRNA gene sequence

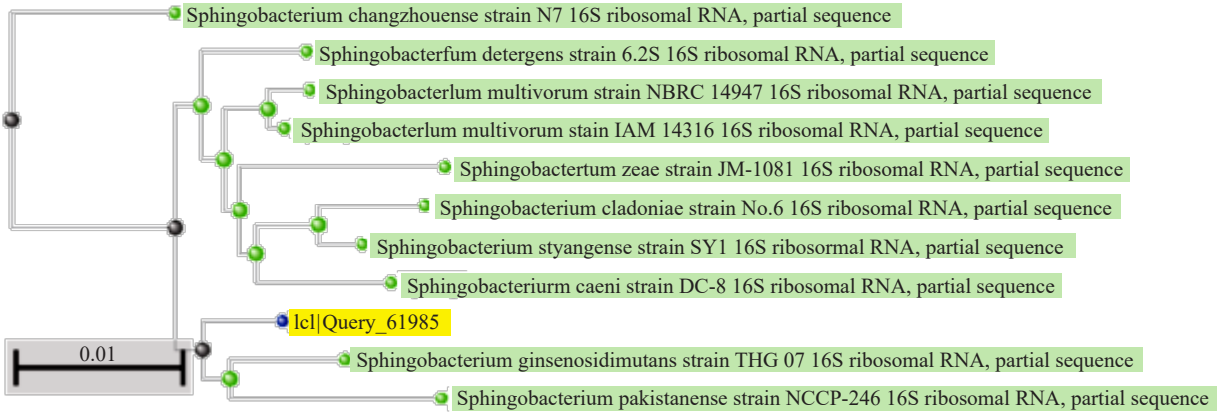


**Figure 8.** Phylogenetic relationship of isolate A6MA-7 and closely related sequences based on partial 16S rRNA gene sequence

Isolate A6MA-7 appeared to have a similarity ratio of 98.57% and was classified with *Sphingobacterium ginsenosidimutans* (NR_108689.1) and *Sphingobacterium pakistanense* (NR_113311.1) but had a closer genetic relationship with *S. ginsenosidimutans*, as clarified in Table 7 and Figure 8. Therefore, isolate A6MA-7 belonged to *S. ginsenosidimutans*.

Isolate MIC-8 has a high similarity ratio of 98.57%, so it is classified with *Kocuria rhizophila* (NR_026452.1) and *Kocuria arsenatis* (NR_148610.1) but has a closer genetic relationship with *Kocuria rhizophila*, as illustrated in Table 7 and Figure 9. Thus, isolate MIC-8 belonged to *K. rhizophila*.

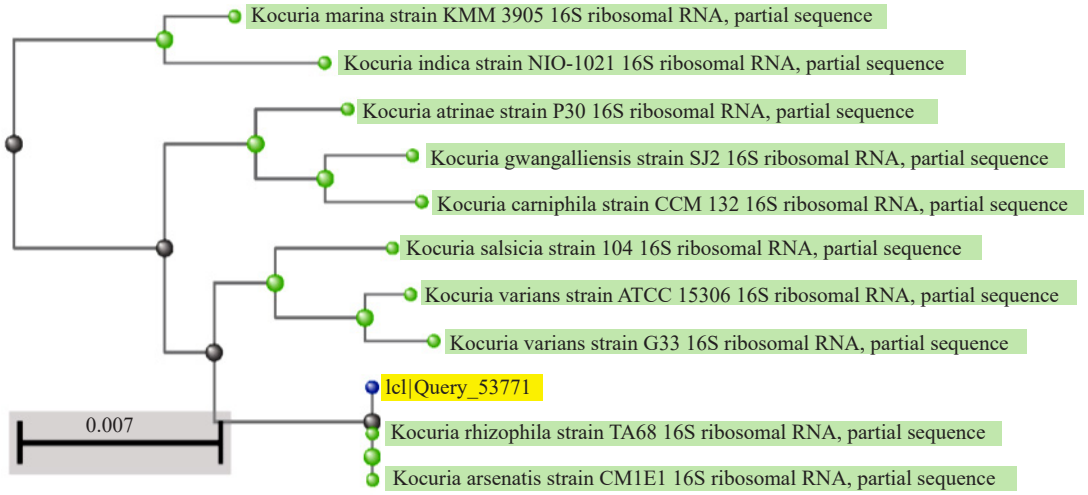


**Figure 9.** Phylogenetic relationship of isolate MIC-8 and closely related sequences based on partial 16S rRNA gene sequence

Although isolate RMA-9 was near to both *Sphingobacterium ginsenosidimutans* (NR_108689.1) and *Sphingobacterium detergens* (NR_118238.1), it was the closest distance to *Sphingobacterium detergens* (NR_118238.1) as appeared in Table 7 and Figure 10. Thus, isolate RMA-9 belongs to *S. detergens*.

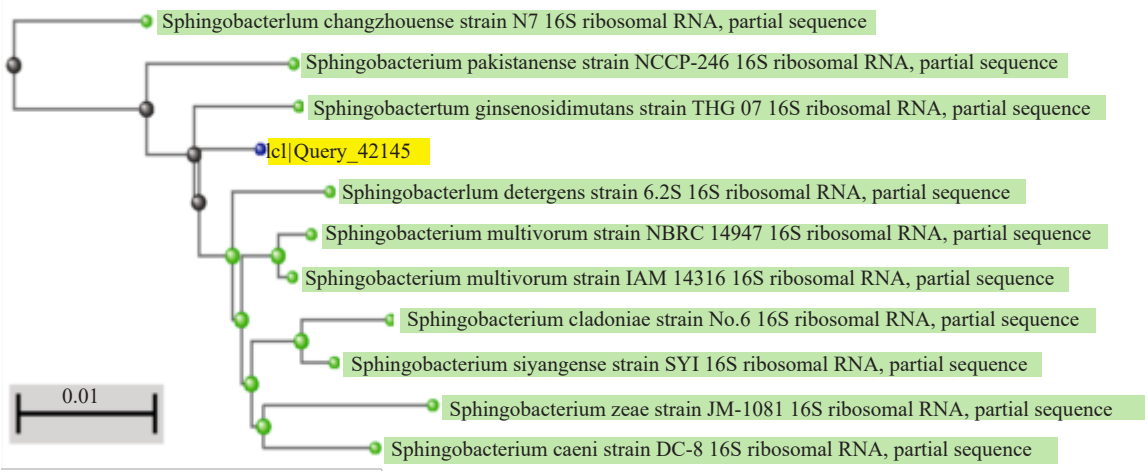


**Figure 10.** Phylogenetic relationship of isolate RMA-9 and closely related sequences based on partial 16S rRNA gene sequence

## 3.2 *Minimum inhibitory concentration of the bacterial isolates against heavy metals*

The results of studies of metal tolerance and growth capabilities in the isolated bacteria revealed high MIC values in bacterial isolates, as shown in Figure 11, indicating high resistance to metals like Cu, Zn, and Ni. Although the original sites did not contain excessive metal concentrations, all isolates showed tolerance at varying levels. It was reported that uncontaminated environments might contain resistant species or adapt to high metal concentrations.[8]

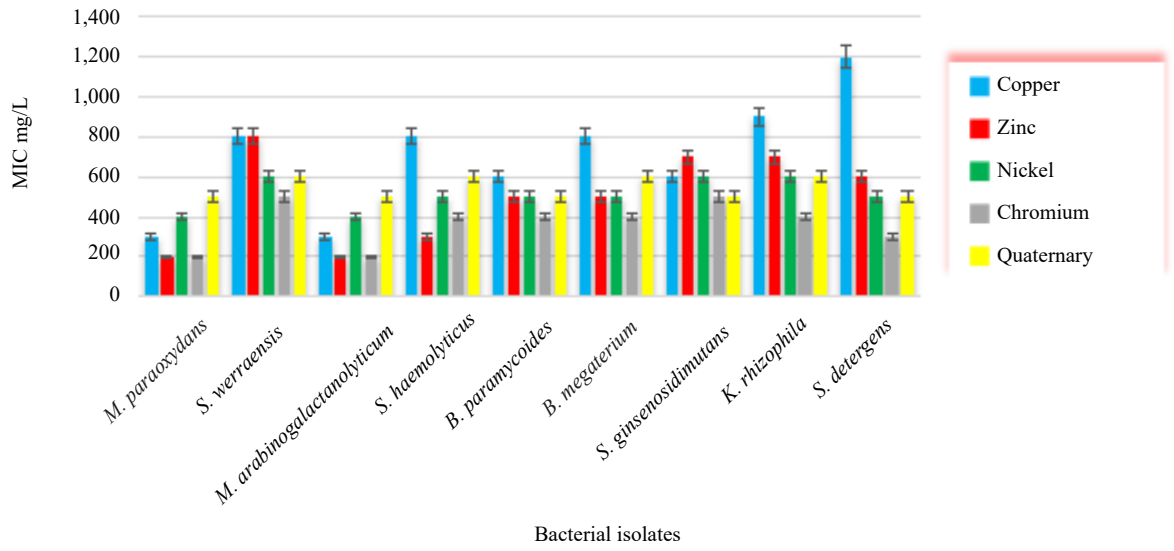


**Figure 11.** Minimum Inhibitory Concentration (MIC) of multimetal resistant bacteria

The study found that the MIC for heavy metals ranged between 200 and 1,200 mg/L. Certain bacteria, including *K. rhizophila*, *S. detergens*, *S. ginsenosidimutans*, and *B. megaterium*, have the highest metal tolerance to heavy metals. This supports previous research indicating that there was prominent metal resistance in bacterial strains isolated from contaminated sites.[78]

It was considered that *Bacillus* sp. is the most effective bacterial species in the processing of heavy metals due to its ability to survive and detoxify metals.[79] *K. rhizophila* showed multiple resistances to heavy metals, as it contains genes associated with tolerance to different concentrations of heavy metals (50 mg/L to 500 mg/L).[80] *Sphingobacterium* spp. achieved the highest specific growth rates in the presence of heavy metals, which indicates its high resistance to heavy metals. The study revealed that *Sphingobacterium* spp., as Gram-negative bacteria, exhibited high copper tolerance due to their complex, three-layered cell wall, which effectively immobilizes metals,[81] unlike the Gram-positive cell wall consisting of a thick peptidoglycan layer.[82]

## 3.3 *Estimation of tolerance and growth of bacterial isolates*

Measuring the optical density per mL (OD = 600) was used to measure the viability of isolates under the action of single and quaternary metals. The results of the effect of metal concentrations of 100 mg/L individually and quaternary on viability are presented in Table 8. The isolates exhibited the ability to grow and tolerate the highest initial metal concentration of 100 mg/L, but there were relatively low optical density values for all compared to the state where no metal is present, which indicated that the growth of bacteria was reduced as a result of that.

**Table 8.** Bacterial density of bacterial isolates at different concentrations of individual metals and quaternary

| Metals Isolates | quaternary | Cr | Ni | Zn | Cu | Control | Mean ± SD |
|---|---|---|---|---|---|---|---|
| *M. paraoxydans* | 0.371 | 0.305 | 0.379 | 0.413 | 0.336 | 0.584 | 0.398 ± 0.098 |
| *S. werraensis* | 0.367 | 0.355 | 0.443 | 0.351 | 0.343 | 0.617 | 0.412 ± 0.107 |
| *M. arabinogalactanolyticum* | 0.381 | 0.295 | 0.394 | 0.409 | 0.325 | 0.575 | 0.397 ± 0.098 |
| *S. haemolyticus* | 0.386 | 0.334 | 0.364 | 0.401 | 0.334 | 0.638 | 0.411 ± 0.114 |
| *B. paramycoides* | 0.350 | 0.301 | 0.380 | 0.373 | 0.304 | 0.672 | 0.397 ± 0.139 |
| *B. megaterium* | 0.437 | 0.413 | 0.391 | 0.396 | 0.360 | 0.686 | 0.439 ± 0.124 |
| *S. ginsenosidimutans* | 0.399 | 0.347 | 0.389 | 0.417 | 0.342 | 0.670 | 0.420 ± 0.125 |
| *K. rhizophila* | 0.413 | 0.367 | 0.442 | 0.460 | 0.352 | 0.635 | 0.442 ± 0.104 |
| *S. detergens* | 0.380 | 0.341 | 0.388 | 0.393 | 0.359 | 0.669 | 0.421 ± 0.122 |

The growth was performed in triplicate, and the findings were expressed as the mean ± Standard Deviation (SD). The results showed a low standard deviation in the data sets, indicating that the data points are generally close to the mean or median value. Where there was less variance in the data points and dispersion below the mean.

## 3.4 *FTIR spectroscopy observation*

Metal-laden biomass from *B. megaterium*, *S. ginsenosidimutans*, and *K. rhizophila* showed obvious peaks in their FTIR spectra; the largest was 3,414.23 $cm^{-1}$, and the smallest was 542.20 $cm^{-1}$. According to the results in three isolates, the peaks matched absorption from N-H, C-H, and O-H single bonds in the range of 4,000-2,500 $cm^{-1}$, which can interact with metal cations. There were distinctive peaks in the 2,000-1,500 $cm^{-1}$ range, which matched absorption from double bonds like C=O, C=N, and C=C. These peaks were in the range of 1,500-400 $cm^{-1}$, and there were also many absorption peaks that represented a wide range of single bonds.

It was evident from the spectra that the bands were shifting and that their intensity was decreasing. All isolates containing single metals and quaternary molecules had FTIR peaks, which provided information on the structure, functional groups, and chemical bonds of the substances causing the interaction, as previously described.[39] Table 9 displays the FTIR absorption wavelengths of each peak along with the corresponding functional groups.

## 3.5 *Co-biosorption from aqueous solution of ions and optimization of adsorption parameters*

The biosorption characteristics of single metals and quaternaries were investigated using single bacteria and a consortium. The effects of certain parameters, like pH, inoculation dose, initial metal concentration, temperature, and contact time, on biosorption were studied. The effects of pH, inoculation dose, and initial metal concentration on biosorption for *K. rhizophila* and a consortium of three isolates (*K. rhizophila*, *B. megaterium*, and *S. ginsenosidimutans*) were assessed at a temperature of 37 °C.

**Table 9.** FTIR peaks and corresponding functional groups

| FTIR peak ($cm^{-1}$) | Functional group assigned |
|---|---|
| 3,415-3,380 | Aromatic primary amine, NH stretch |
| 3,400-3,300 | Alcohol, hydroxyl compound- OH- Stretch and NH stretching of the protein |
| 2,935-2,915 | Methylene C-H |
| 1,670-1,640 | Carboxylic groups |
| 1,680-1,630 | Carbonyl compound, amide |
| 1,500-1,600 | Carboxylic groups and N-H |
| 1,300-1,450 | C-O stretch |
| 1,150-950 | $PO_4^{-3}$ stretching |
| 1,090-1,020 | Primary amino, CN stretch primary amine |
| 900-670 | Aromatic C-H |
| 800-700 | Aliphatic chloro compound C-Cl (Alkyl halides) |
| 500-700 | Phosphate or sulphate functional groups |

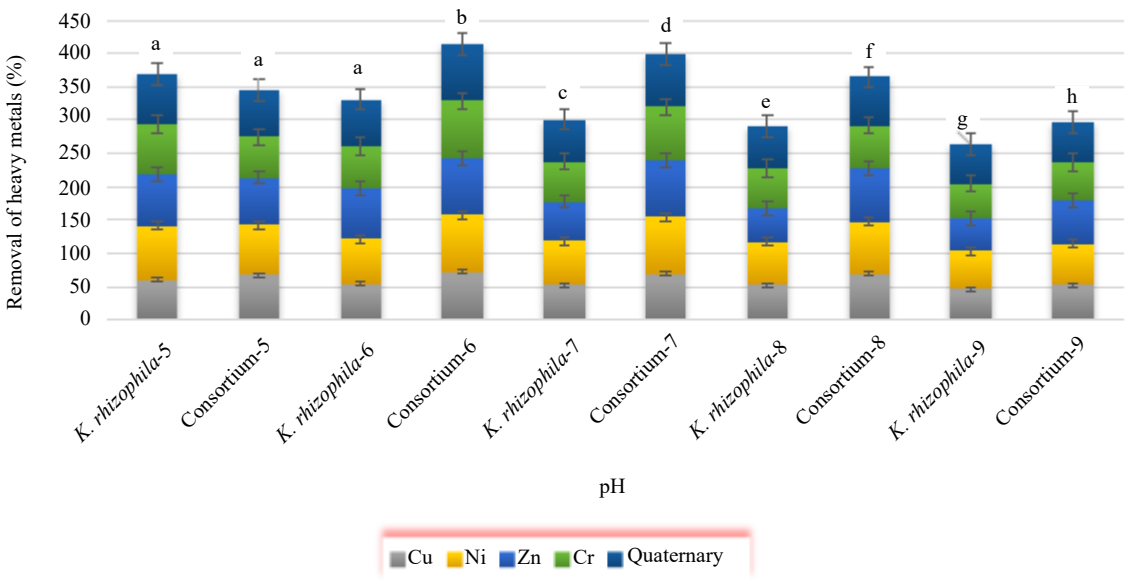


**Figure 12.** Effect of pH on metals biosorption by *K. rhizophila* and consortium
*Values with different superscript letters are statistically significant ($p \leq 0.05$)

The results illustrated that there was variation in metal biosorption by the biomass of single and consortium with differences in pH values. With increasing pH, the rate of biosorption decreased until it reached its maximum value of pH 9.0. In both single and consortium systems, the optimal metal concentration was at a minimum concentration of 10 mg/L. The maximum biosorption for all the metals with *K. rhizophila* and the consortium was obtained after 50 min. This was set as an equilibrium time, and there was no significant change ($P \geq 0.05$) in metal biosorption after 50 min, although all

the experiments were carried out for up to 70 min. This implies that the biosorbent types were saturated at around 50, and 60, or 70 min. For inoculation dose and temperature, metal biosorption increased at the inoculation dose of 2.0% with *K. rhizophila* and 1.5% with the consortium, and then decreased after levelled off. The biosorption of metal ions also increased with temperature up to 37 °C, but decreased between 42 and 50 °C.

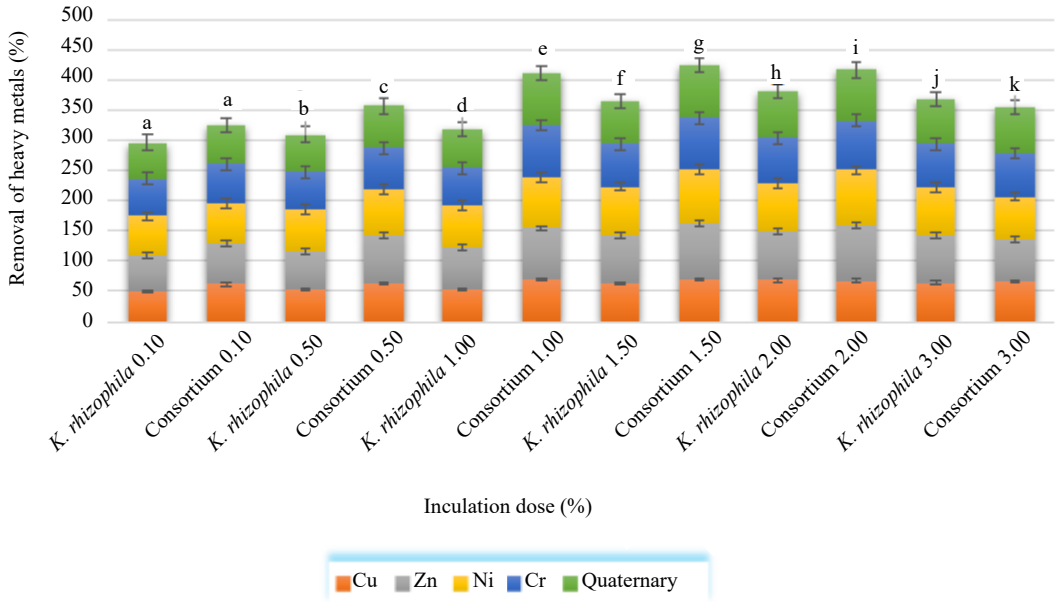


**Figure 13.** Effect of inoculation dose on metals biosorption by *K. rhizophila* and consortium
*Values with different superscript letters are statistically significant ($p \leq 0.05$)

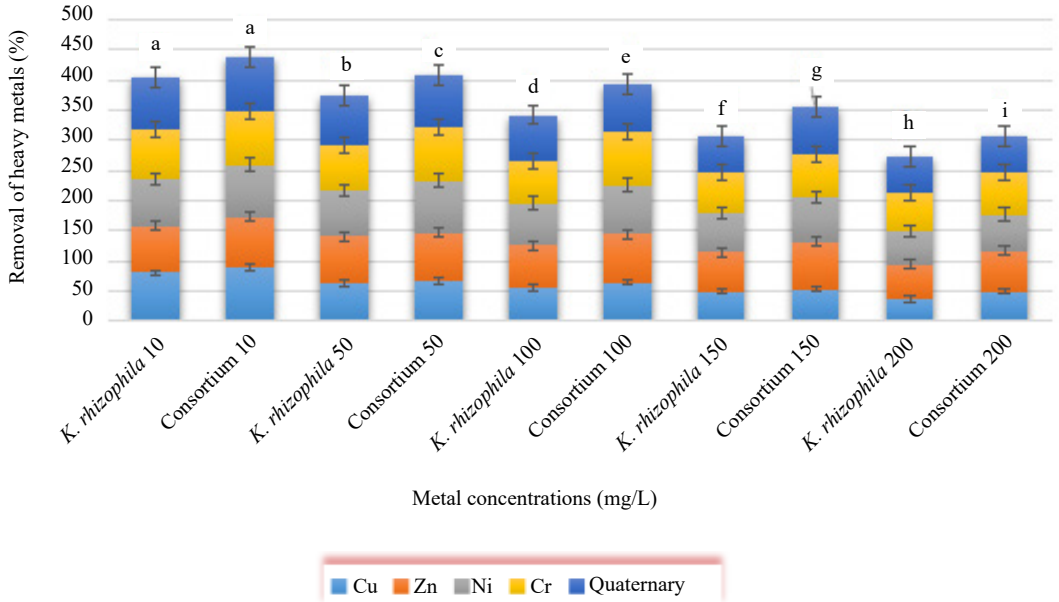


**Figure 14.** Effect of metal concentrations on biosorption by *K. rhizophila* and consortium
*Values with different superscript letters are statistically significant ($p \leq 0.05$)

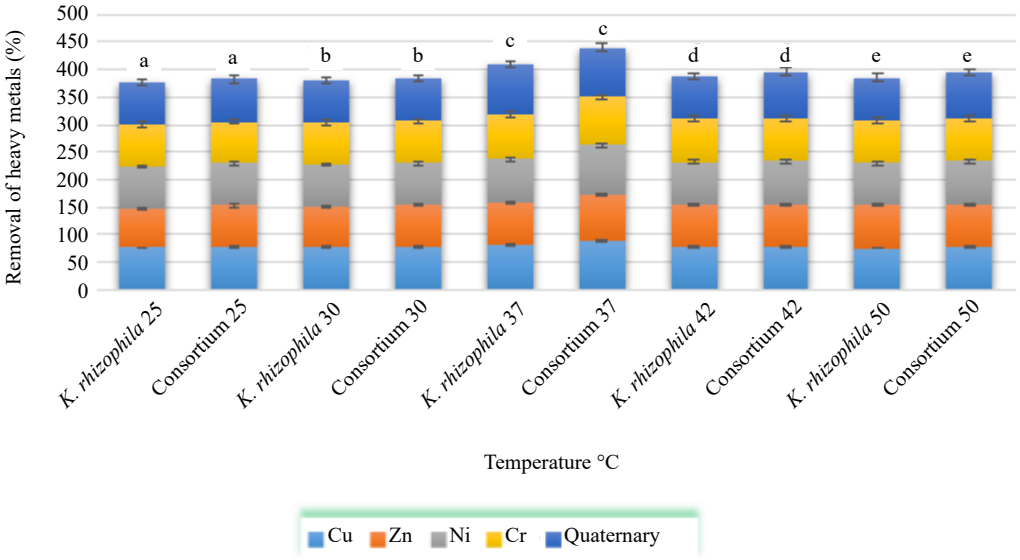


**Figure 15.** Effect of temperature on metals biosorption by *K. rhizophila* and consortium
*Values with different superscript letters are statistically significant ($p \leq 0.05$)

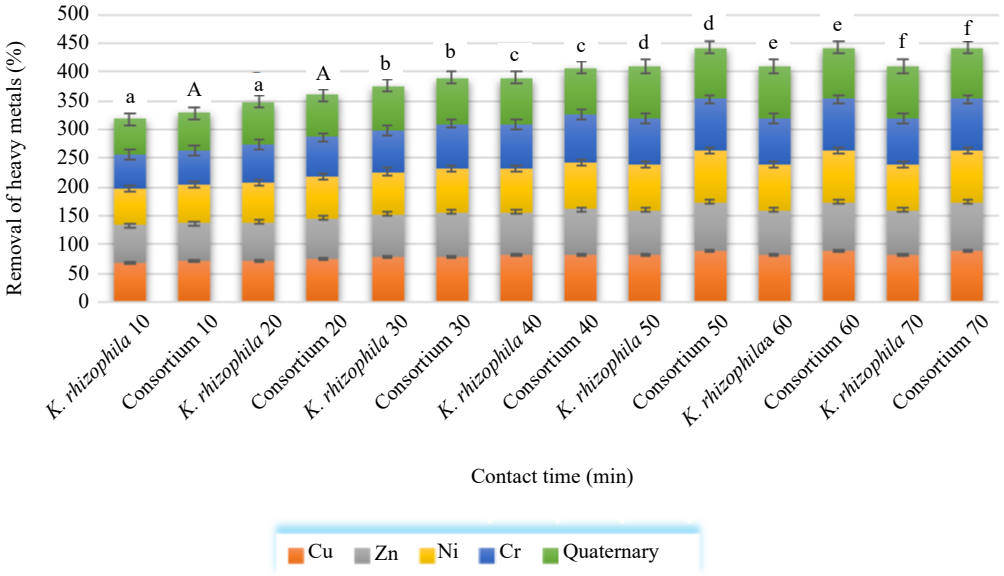


**Figure 16.** Effect of contact time on metals biosorption by *K. rhizophila* and consortium
*Values with different superscript letters are statistically significant ($p \leq 0.05$)

The summary of results showed that the optimum pH, inoculation dose, and initial metal concentration values for *K. rhizophila* biosorption were found to be 5, 2%, and 10 mg/L, at 50 min, respectively. Whereas the optimum pH of the consortium (*K. rhizophila*, *B. megaterium*, and *S. ginsenosidimutans*) was 6, and the biomass dosage and initial metal concentration of the consortium were 1.5% and 10 mg/L respectively. The equilibrium time was achieved after 50 min in both single and consortium bacteria at 37 °C.

The results of the statistical analysis indicated that there was a difference ($P \geq 0.05$) in the optimum parameters of biosorption between *K. rhizophila* and a consortium of three isolates. Details of the results of all parameters and the statistical analysis are presented in Figures 12-16.

## 3.6 *Modelling and calculation of metal biosorption equilibrium parameters*

Adsorption equation modeling predicts adsorption coefficients and efficiencies. Various models have been used to explain the interaction of metals in both single-component and multicomponent systems. Multicomponent adsorption equation models have connected how much metal can be absorbed to the amounts of other metals in the wastewater and have forecasted how these interactions happen, where the equilibrium sorption of a single isolate and a consortium was estimated.

The equilibrium sorption data were fitted into Langmuir, Freundlich, Temkin, and Dubinin-Radushkevich (DRK) isotherms to understand the mechanism of metal adsorption by bacterial isolates. The evaluated biosorption isotherm parameters and their results are presented in Table 10, and the plot of all equilibrium adsorption isotherms used in this study for single bacteria and consortium are shown in Figures 17 and 18. The Langmuir isotherm had the highest $R^2$ value, while the Freundlich equation better represented copper biosorption by the consortium. Experimental data agreed with the Langmuir model for single and quaternary metals with good correlation coefficients $R^2$ of 0.99.

**Table 10.** Isothermal parameters for the biosorption of heavy metals onto *K. rhizophila* and consortium

| Adsorbate | Copper | | Nickel | | Zinc | | Chromium | | Quaternary | |
|---|---|---|---|---|---|---|---|---|---|---|
| Adsorbents | *K. rhizophila* | consortium | *K. rhizophila* | consortium | *K. rhizophila* | consortium | *K. rhizophila* | consortium | *K. rhizophila* | consortium |
| Isothermal parameters | Langmuir | | | | | | | | | |
| $q_{max}$ (mg/g) | 8.13 | 8.16 | 26.88 | 33.11 | 21.65 | 22.42 | 18.66 | 28.81 | 11.75 | 21.28 |
| $K_L$ (L/mg ) | 0.069 | 0.130 | 0.014 | 0.017 | 0.019 | 0.034 | 0.026 | 0.031 | 0.084 | 0.046 |
| $R^2$ | 0.995 | 0.982 | 0.998 | 0.999 | 0.999 | 0.999 | 0.999 | 0.997 | 0.996 | 0.999 |
| $R_L$ | 0.591 | 0.434 | 0.877 | 0.854 | 0.840 | 0.746 | 0.793 | 0.763 | 0.543 | 0.684 |
| | Freundlich | | | | | | | | | |
| $n$ | 1.967 | 1.869 | 1.492 | 1.565 | 1.522 | 1.605 | 1.426 | 1.556 | 1.663 | 1.450 |
| $K_f$ (mg/g) $(L/mg)^{1/n}$ | 1.587 | 1.090 | 1.973 | 1.241 | 1.938 | 1.421 | 2.107 | 1.698 | 1.077 | 1.310 |
| $R^2$ | 0.987 | 0.983 | 0.983 | 0.945 | 0.983 | 0.954 | 0.998 | 0.916 | 0.980 | 0.977 |
| | Temkin | | | | | | | | | |
| $B$ | 1.88 | 2.124 | 3.292 | 4.043 | 3.149 | 3.109 | 3.494 | 3.390 | 2.769 | 3.650 |
| $K_T$ (L/g) | 2.26 | 1.009 | 13.33 | 11.285 | 10.728 | 1.769 | 13.185 | 1.168 | 6.672 | 1.368 |
| $R^2$ | 0.944 | 0.885 | 0.968 | 0.930 | 0.965 | 0.901 | 0.899 | 0.965 | 0.900 | 0.952 |
| | Dubinin-Radushkevich | | | | | | | | | |
| $q_s$ (mg/g) | 1.322 | 1.195 | 1.411 | 1.319 | 1.298 | 2.312 | 1.318 | 1.258 | 1.209 | 1.219 |
| $K_{ad}$ ($mol^2/kJ^2$) | $1 \times 10^{-7}$ | $5 \times 10^{-8}$ | $2 \times 10^{-7}$ | $1 \times 10^{-7}$ | $1 \times 10^{-7}$ | $6 \times 10^{-8}$ | $1 \times 10^{-7}$ | $8 \times 10^{-7}$ | $4 \times 10^{-8}$ | $7 \times 10^{-8}$ |
| $E$ (kJ/mol) | 2.236 | 3.162 | 1.581 | 2.236 | 2.236 | 2.887 | 2.236 | 7.908 | 3.536 | 2.773 |
| $R^2$ | 0.912 | 0.890 | 0.966 | 0.990 | 0.978 | 0.838 | 0.953 | 0.998 | 0.983 | 0.934 |

The results showed that the maximum biosorption capacity ($q_m$) of *K. rhizophila* and the consortium was found to be 26.88 mg/g and 33.1 mg/g of nickel, respectively. The free energy values in both *K. rhizophila* and the consortium obtained from the D-R isotherm were less than 8 kJ/mol. Moreover, the $K_L$ (the Langmuir biosorption constant (L/mg) related to the free energy of biosorption) was found to be 0.014 L/mg and 0.017 L/mg.

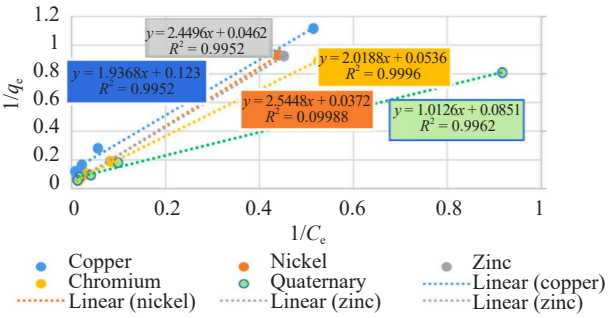


Langmuir isotherm for different metals biosorption onto *K. rhizophila*

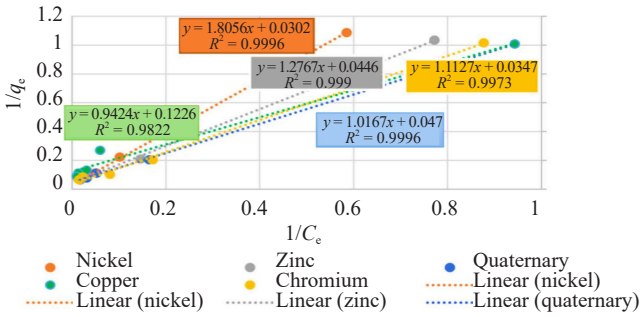


Langmuir isotherm for different metals biosorption onto consortium

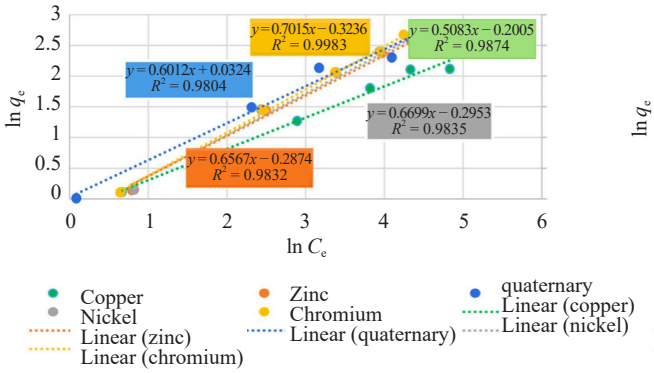


Freundlich isotherm for different metals biosorption onto *K rhizophila*

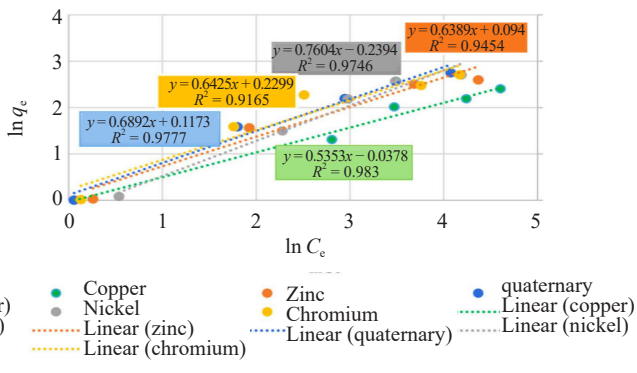


Freundlich isotherm for different metals biosorption onto consortium

**Figure 17.** Results of other equilibrium biosorption equations for both a consortium and a single bacterium

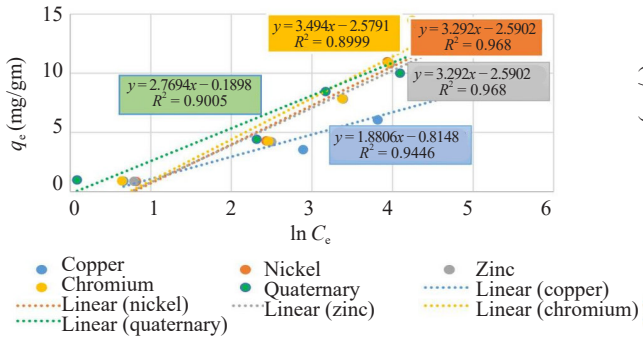


Temkin isotherm for different metals biosorption onto *K rhizophila*

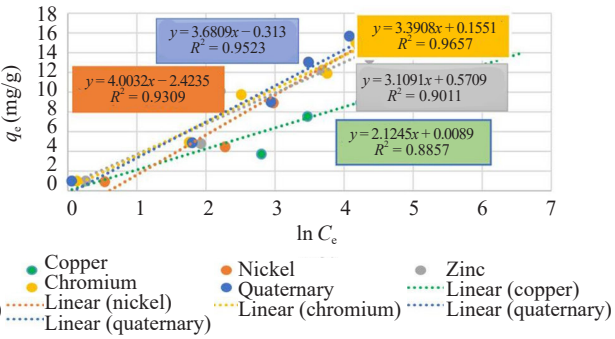


Temkin isotherm for different metals biosorption onto consortium

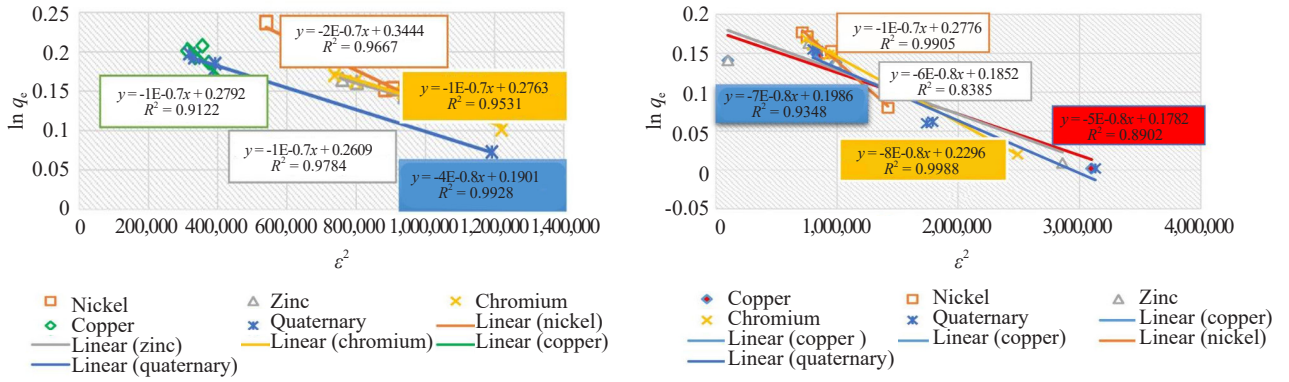


Dubinin isotherm for different metals biosorption onto *K rhizophila*

Dubinin isotherm for different metals biosorption onto consortium

**Figure 18.** Results of other equilibrium biosorption equations for both a consortium and a single bacterium

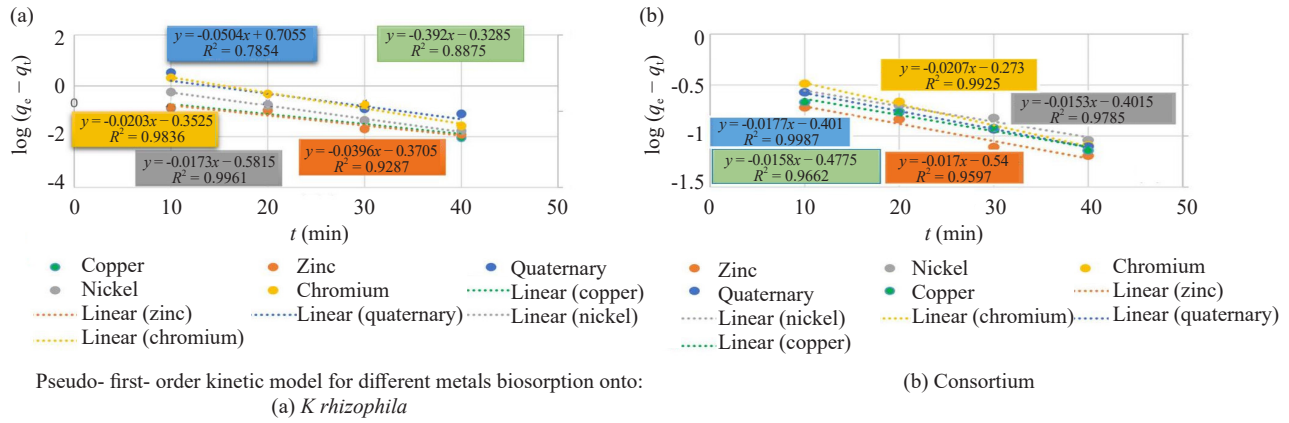


Pseudo- first- order kinetic model for different metals biosorption onto: (a) *K rhizophila*

(b) Consortium

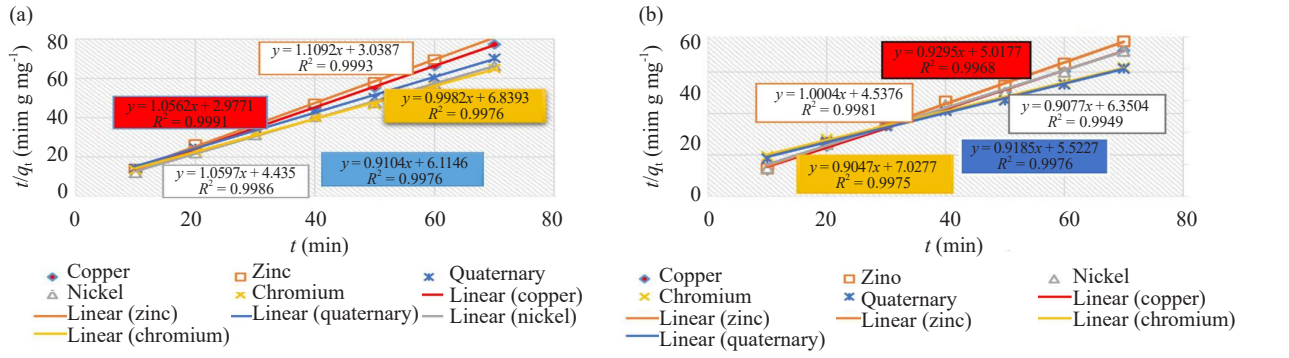


Pseudo- second- order kinetic model for different metals biosorption onto: (a) *K rhizophila*

(b) Consortium

**Figure 19.** Results of other kinetic biosorption equations for both consortia and single bacterium

The $Q_{max} = q_m$ (the maximum monolayer biosorption capacity of the biosorbent, mg/g). The $q_m$ values calculated from the Langmuir model were larger than those of a previous study performed with *Kocuria* sp. BRI 36, which was 10.41 mg/gm for Ni. This result was considered as an indicator of the effectiveness of *Kocuria* sp. BRI 36 biomass as a potential biosorbent for treatment of $Ni^{2+}$ and $Cr^{3+}$ contaminated aquatic sites.[83]

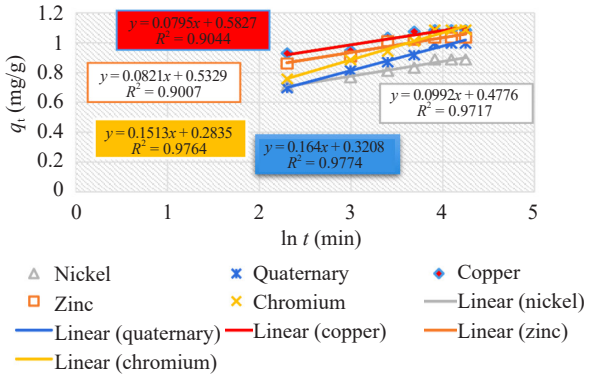


Elovich kinetic model for different metals biosorption onto *K rhizophila*

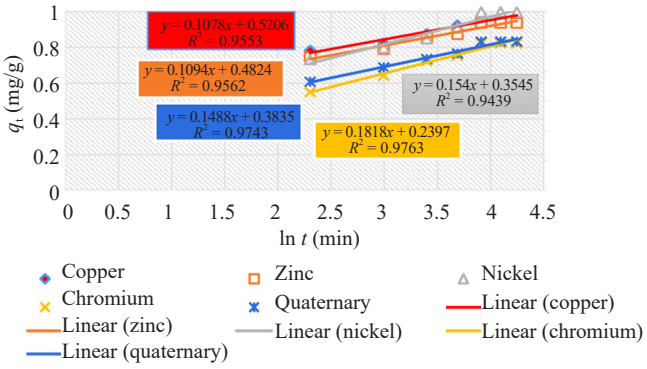


Elovich kinetic model for different metals biosorption onto consortium

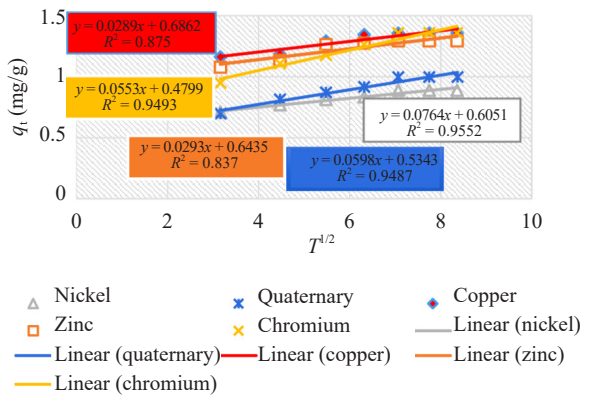


Intraparticle diffusion kinetic model for different metals biosorption onto *K rhizophila*

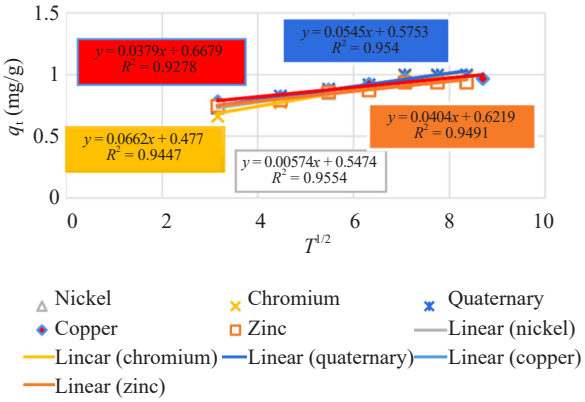


Intraparticle diffusion kinetic model for different metals biosorption onto consortium

**Figure 20.** Results of other kinetic biosorption equations for both consortia and single bacterium

## 3.7 *Kinetics study*

The kinetic mechanism of biosorption was analyzed using the pseudo-first-order, pseudo-second-order, Elovich model, and intra-particle diffusion. The kinetic parameters and kinetic models that were applied to the biosorption data are presented in Table 11. Plotting the experimental data obtained is shown in Figures 19 and 20. From four models, the pseudo-second-order presented a very good fit ($R^2 \geq 0.99$) for the biosorption of all single metals compared to the pseudo-first-order model, but did not provide good fits for quaternary on consortium, as the $R^2$ value was more with pseudo-first-order than pseudo-second-order. Furthermore, the value of $q_e$ calculated from the pseudo-second-order model was close to the experimental value, supporting the validity of this model for the biosorption of single and quaternary metals. This showed the pseudo-second-order model best describes the biosorption of single metals (Cu, Zn, Ni, and Cr), indicating chemisorption. However, the pseudo-first-order model best describes quaternary indicating physisorption.

The parameters of kinetics showed that the initial sorption rate ($h$) of single metals onto a single isolate was better for Cu, followed by Zn and Ni. As well, the initial sorption rates of Cu and quaternary were better on the consortium. Furthermore, the amounts of single metals such as copper, zinc, and nickel were highly adsorbed in quaternary solutions by *K. rhizophila* and a consortium of three isolates, *B. megaterium*, *S. ginsenosidimutans*, and *K. rhizophila*. Only the adsorption of chromium was slightly lower in the quaternary solution.

**Table 11.** Kinetic biosorption parameters for heavy metals ions onto *K. rhizophila* and consortium

| Adsorbate | Copper | | Zinc | | Nickel | | Chromium | | Quaternary | |
|---|---|---|---|---|---|---|---|---|---|---|
| Adsorbents | *K. rhizophila* | consortium | *K. rhizophila* | consortium | *K. rhizophila* | consortium | *K. rhizophila* | consortium | *K. rhizophila* | consortium |
| Parameters Kinetic: $q_e$ exp (mg/g) | 0.905 | 0.996 | 0.862 | 0.936 | 0.888 | 0.998 | 0.906 | 0.986 | 0.996 | 0.998 |
| Pseudo-first-order | | | | | | | | | | |
| $q_e$ cal (mg/g) | 2.130 | 3.00 | 2.347 | 3.467 | 3.815 | 2.520 | 2.251 | 1.874 | 5.076 | 2.518 |
| $K_1$ ($min^{-1}$) | 0.090 | 2.09 | 0.091 | 1.851 | 0.0398 | 2.490 | 0.047 | 3.663 | 0.1161 | 2.493 |
| $R^2$ | 0.887 | 0.966 | 0.929 | 0.959 | 0.996 | 0.979 | 0.983 | 0.992 | 0.785 | 0.999 |
| Pseudo-second-order | | | | | | | | | | |
| $q_e$ cal (mg/g) | 0.947 | 1.076 | 0.901 | 0.999 | 0.943 | 1.101 | 1.001 | 1.105 | 1.098 | 1.088 |
| $K_2$ (g/mg min) | 0.374 | 0.199 | 0.404 | 0.220 | 0.253 | 0.157 | 0.146 | 0.142 | 0.136 | 0.181 |
| $h$ (mg/g min) | 0.335 | 0.230 | 0.328 | 0.220 | 0.225 | 0.190 | 0.146 | 0.173 | 0.163 | 0.214 |
| $R^2$ | 0.999 | 0.997 | 0.999 | 0.998 | 0.999 | 0.995 | 0.998 | 0.998 | 0.998 | 0.998 |
| Elovich model | | | | | | | | | | |
| $\alpha$ (mg/g·min) | 121.14 | 13.49 | 54.109 | 9.03 | 12.219 | 1.539 | 1.015 | 1.471 | 1.159 | 1.751 |
| $\beta$ (g/mg) | 12.579 | 9.276 | 12.180 | 9.140 | 10.080 | 6.493 | 6.609 | 5.500 | 6.098 | 6.720 |
| $R^2$ | 0.904 | 0.955 | 0.901 | 0.956 | 0.971 | 0.943 | 0.976 | 0.907 | 0.977 | 0.974 |
| Intraparticle diffusion | | | | | | | | | | |
| $K_{int}$ (mg/g $min^{1/2}$) | 0.029 | 0.038 | 0.029 | 0.040 | 0.036 | 0.057 | 0.055 | 0.066 | 0.059 | 0.054 |
| $C_i$ | 0.686 | 0.668 | 0.643 | 0.621 | 0.605 | 0.547 | 0.479 | 0.477 | 0.534 | 0.575 |
| $R^2$ | 0.875 | 0.928 | 0.837 | 0.949 | 0.955 | 0.955 | 0.949 | 0.944 | 0.949 | 0.954 |

## 3.8 *Biosorption thermodynamics*

To describe the biosorption thermodynamic behavior of single metals and quaternary metals on *K. rhizophila* and consortium biomass, the parameters of thermodynamic, including changes in free energy ($\Delta G$), enthalpy ($\Delta H$), and entropy ($\Delta S$), for single and quaternary biosorption, were evaluated. The results of thermodynamics parameters and the application of biosorption data by single bacteria and a consortium are shown in Tables 12 and 13 and Figures 21 and 22.

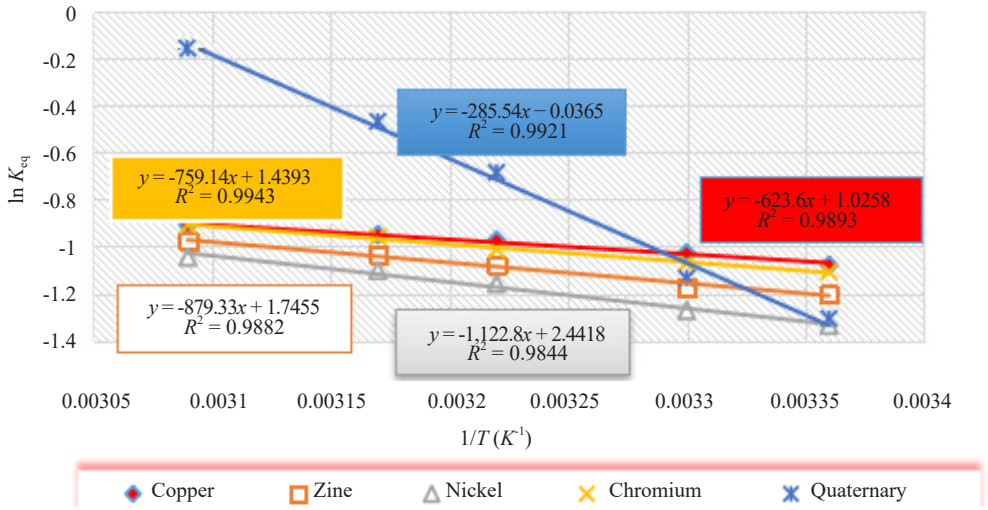


**Figure 21.** Thermodynamic parameters for different metals biosorption onto *K. rhizophila*

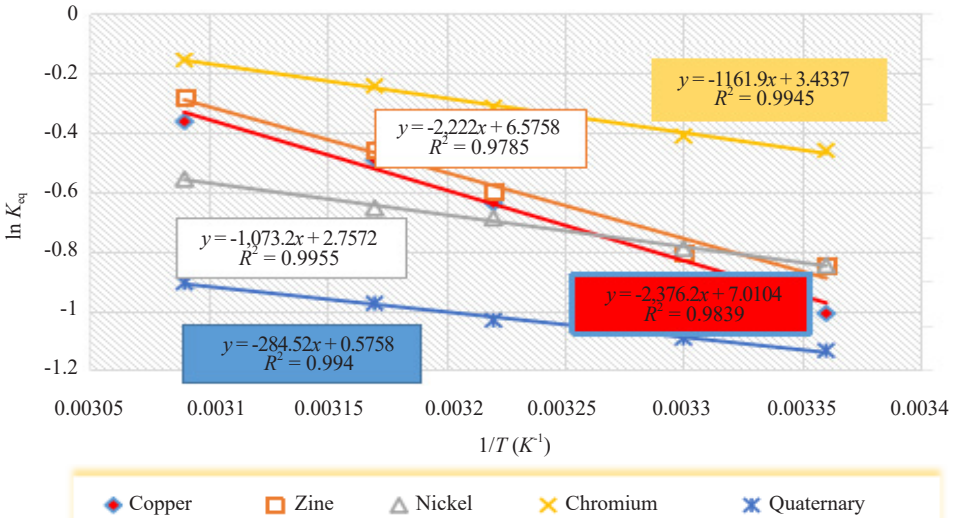


**Figure 22.** Thermodynamic parameters for different metals biosorption onto consortium

**Table 12.** Thermodynamics parameters for biosorption of heavy metals ions onto *K. rhizophila* at the different temperatures

| Metals parameters | Copper | Zinc | Nickel | Chromium | Quaternary |
|---|---|---|---|---|---|
| $\Delta H°$ kJ/mol | 5.18 | 7.31 | 9.33 | 6.31 | 2.37 |
| $\Delta S°$ J/mol | 8.52 | 14.51 | 20.30 | 11.97 | 0.303 |
| $\Delta G°$ kJ/mol at: | | | | | |
| 25 °C | -2.53 | -4.31 | -6.04 | -3.56 | -87.92 |
| 30 °C | -2.58 | -4.39 | -6.14 | -3.62 | -89.43 |
| 37 °C | -2.63 | -4.49 | -6.28 | -3.71 | -91.56 |
| 42 °C | -2.68 | -4.56 | -6.39 | -3.76 | -93.08 |
| 50 °C | -2.74 | -4.68 | -6.54 | -3.86 | -95.49 |

**Table 13.** Thermodynamics parameters for biosorption of heavy metals ions onto consortium at the different temperatures

| Metals parameters | Copper | Zinc | Nickel | Chromium | Quaternary |
|---|---|---|---|---|---|
| $\Delta H°$ kJ/mol | 19.76 | 18.47 | 8.92 | 9.66 | 2.37 |
| $\Delta S°$ J/mol | 58.28 | 54.67 | 22.92 | 28.54 | 4.79 |
| $\Delta G°$ kJ/mol at: | | | | | |
| 25 °C | -17.34 | -16.27 | -6.83 | -8.49 | -1.42 |
| 30 °C | -17.63 | -16.54 | -6.93 | -8.63 | -1.44 |
| 37 °C | -18.04 | -16.92 | -7.09 | -8.83 | -1.48 |
| 42 °C | -18.33 | -17.20 | -7.21 | -8.98 | -1.50 |
| 50 °C | -18.80 | -17.63 | -7.39 | -9.20 | -1.54 |

## 4. Discussion

The electroplating effluent samples were inoculated into shake flasks of enrichment media containing nutrient agar combined with metal ions to isolate bacterial strains. The nine isolates out of sixty that were most tolerant to metals were examined. Biochemical tests of the isolates were performed to confirm their authenticity, and 16S rRNA molecular sequence examination and phylogenetic analysis were performed to identify nine isolates at the species level. As well as a genomic DNA extraction pattern with a determination of similarity rate that was 98-100%. Then, nucleotide sequences were deposited in NCBI databases. The obtained results showed the taxonomic diversity in contaminated samples, which supports the fact that a variety of bacteria can adapt to high amounts of heavy metal contamination.[84-86]

The study explored the metal tolerance and growth properties of nine bacterial isolates. The isolated bacteria can grow in single and multiple mineral solutions up to 100 mg/L. Minimum Inhibitory Concentration (MIC) assays of the isolates showed different and high metal tolerance abilities. The isolates showed a higher tolerance to multiple metals (quaternary metals) and were more clearly tolerant to copper.

The study examined the biosorption characteristics and the effects of parameters like pH, inoculation dose, and initial metal concentration on biosorption for *K. rhizophila* and a consortium of three isolates (*K. rhizophila*, *B. megaterium*, and *S. ginsenosidimutans*). The results found that metal biosorption varied by biomass type and pH value. That is because high pH leads to the precipitation of metal hydroxides, causing metal ions to become immobilized. Also, at low pH, heavy metals tend to form free ionic species; thus, more hydrogen ions become available to saturate the metal binding sites. As a result, the biosorption surface may be positively charged at an acidic pH, resulting in reduced attraction between the biosorbent and the metal cations.[87] Because of the limited number of binding sites created by the increase in initial metal concentration, increasing metal concentration reduced biosorption more in single bacteria than in consortium.

In previous research on *K. rhizophila*, the results of the parameters studied indicated that a pH range of 4.0-6.0 could achieve the biosorption mechanism.[75] In addition, it was found that the optimum pH range for most bacteria is 5.5-6.5.[56] In the current study, it was shown that co-biosorption of *K. rhizophila* and consortium achieved biosorption rates ranging between 77.3-89.1% and 82.9-89.4%, respectively; this is consistent with metal removal in the range of 60–95%, which was published earlier by Mulik et al.[83]

The optimal metal concentration for single and consortium systems was 10 mg/L, with maximum biosorption after 50 minutes. There was no significant change in metal biosorption after 50 minutes, suggesting biosorbent types are saturated at 50, 60, or 70 minutes. Thus, during these times, all active sites are occupied and not available for further metal ion biosorption. In addition, the findings showed that mineral absorption increased with increasing inoculation dosage up to 2.0% (0.898 gm) with *K. rhizophila* and 1.5% (0.9 gm) with the consortium, then leveled off. This may be due to the lack of adsorption sites due to their overlap with the increase in biomass, or the sites may become limited

with increasing inoculation dosage, causing the adsorption of ions to decline.[73]

It was also shown that the biosorption of metal ions increased with temperature up to 37 °C but decreased between 42 and 50 °C, which may be attributed to the fact that increasing temperature led to damage to the active sites on the bacterial cell surface and a reduction of binding sites.[88] The greater biosorption was at the lowest initial concentration of each metal due to the fast mineral uptake capacity of bacterial biomass, whereas the lack of surface binding sites or saturation of the biosorbent surface may explain the decrease in biosorption at high metal concentrations. The results illustrated that *K. rhizophila* and the consortium achieved high biosorption at 37 °C, and then decreased with increasing temperatures. As previously mentioned, high temperatures may reduce the ability of bacterial biomass to absorb ions such as $Cu^{2+}$ and $Zn^{2+}$ due to a decrease in bacterial metabolism and the destruction of active binding sites on bacterial cells.[89]

The results of a previous study found that the optimum contact time for *K. rhizophila* and other species of *Kocuria* sp. was in the range of 60-80 min,[90] and biomass concentration was between 1% and 0.8% of the same isolate, which demonstrates the best performance as a biosorbent at this range in the literature.[83,87] The results of the current study found that the contact time in a single isolate was less and the biomass concentration was higher compared to previous research, confirming the earlier reported fact that the rapid equilibrium time being reached can be attributed to a lot of binding sites on the surface of the single biomass, which was the highest, and also to consortium.[91] The binding sites became occupied and then levelled off after 50 min. As well as the fact that the variance in the time required to attain equilibrium in the solution depends on the biosorbent.[87]

There was a difference in the biosorption of single and quaternary metals by single bacteria and consortium. This is because the microbial consortium consists of different isolates with different properties and abilities that can absorb different metals. These microbial members of the consortium interact positively with each other in a cooperative manner that leads to more effective metal biosorption. The results determined that optimum values of each parameter can be used for modelling the co-biosorption of metals onto bacteria. It was reported that consortiums of cultures are metabolically superior for the biosorption of metals and are more appropriate for field applications of metals.[92]

A statistical analysis of the effects of different parameters on co-biosorption revealed a significant difference between the consortium and *K. rhizophila* at pH 5 and 6 versus pH 7, 8, and 9. In general, the pH of the consortium differs significantly from *K. rhizophila* at high pH. The inoculation doses of *K. rhizophila* (0.5%, 1.0%, 1.5%, 2.0%, and 3.0%) were significantly different with the same dose of consortium. There was a significant difference between *K. rhizophila* and the consortium at metal concentrations of 50 mg/L, 100 mg/L, 150 mg/L, and 200 mg/L. The temperatures of 25 and 30 °C in both the consortium and *K. rhizophila* differed significantly from the others, as did the contact times of 10 and 20 min, which were also significantly different from the rest of the tested periods.

## 4.1 *Modelling and calculation of metal biosorption equilibrium parameters*

Adsorbent efficiency and metal removal ability could be quantitatively compared using adsorption isotherm modeling to predict the adsorption parameters.[29] As a result, equilibrium adsorption isotherm data are essential for constructing adsorption systems.[93] Several adsorption isotherm models, including Langmuir, Freundlich, Dubinin-Radushkevich, and Temkin, as well as kinetic models such as pseudo-first-order, pseudo-second-order, Elovich, and Webber-Morris intra-particle diffusion, have been used to explain the interactive effect between metals and adsorbents in single-component systems.[29,94,95]

However, real wastewater contains a range of chemicals that cause competition and interaction among the contaminants. The single-component isotherm models are frequently modified and applied to multicomponent systems. This is due to the complex mechanism involved in multicomponent absorption, which necessitates the use of more complex models. To determine the interaction of the contaminants in the system and with the adsorbent, several isotherm equations used for single-component systems are converted to systems of multicomponent.[96] Multicomponent adsorption isotherm models significantly help correlate the absorption capability of one metal with the equilibrium concentration of the other coexisting metal concentrations in the effluent.

The competitive adsorption isotherm models could predict the types of interactions and demonstrate the various forms of interactions between heavy metal ions in a multicomponent sorption system at equilibrium.[29]

The study estimated the equilibrium sorption of a single isolate, *K. rhizophila* and a consortium of three isolates, *K. rhizophila*, *B. megaterium*, and *S. ginsenosidimutans* using Langmuir, Freundlich, Temkin and Dubinin-Radushkevich

isotherms, revealing the mechanism of metal adsorption by bacteria. The Langmuir isotherm had the highest $R^2$ value. Only one case, the biosorption of copper by the consortium, was better represented by the Freundlich equation. That implied that the surface of the consortium was heterogeneous and multilayer for copper adsorption was heterogeneous and multilayer for copper adsorption and biosorption. The experimental data were in good agreement with the Langmuir model for single metals (Zn, Ni, and Cr) and quaternary metals, with good correlation coefficients $R^2$ of 0.99. The applicability of Langmuir isotherms to remove metal ions by the single isolate and consortium indicated that the adsorption process occurred in a monolayer coverage method without interaction between the adsorbed ions with each other. In addition, the active adsorption sites were homogeneously distributed on the surface of the adsorbent and were identical for all ions. Thus, each active site is bound to only one ionic metal.

The free energy values in both *K. rhizophila* and the consortium obtained from the D-R isotherm were less than 8 kJ/mol; thus, type adsorption can be considered a physisorption process. Although this model showed the highest correlation coefficient ($R^2$) value of 0.998 compared to other models when Cr was adsorbed by a consortium, the adsorption capacity was the lowest, as the adsorption was best with Langmuir isotherms. It was also found that the affinity of the biosorbent to sorbate ($R_L < 1$) indicated favorable sorption. The results showed that the maximum biosorption capacity ($q_m$) of *K. rhizophila* and the consortium was with nickel. Compared to one of the results, the ($q_m$) values calculated from the Langmuir model were larger than those of a previous study performed with *Kocuria* sp. BRI 36, which was 10.41 mg/gm for Ni. This result was considered an indicator of the effectiveness of *Kocuria* sp. BRI 36 biomass as a potential biosorbent for the treatment of $Ni^{2+}$ and $Cr^{3+}$ contaminated aquatic sites.[83]

## 4.2 *Comparative analysis of the biosorption models used in the study*

In the current study, the adsorption equilibrium of a substance on a surface at a given temperature was explained by the Langmuir, Freundlich, Temkin, and Dubinin-Radushkevich (D-R) adsorption models. The Langmuir isotherm assumes homogeneity of the biosorption process, i.e., uniform biosorption energy with no migration of ions in the surface plane of the biosorbent molecules used, with monolayer coverage and uniform biosorption energies.[97] The linear Langmuir isotherm is displayed in Table 1. Whereas the model of the Freundlich biosorption isotherm suggested that metal ion uptake takes place on a heterogeneous surface by multilayer biosorption with the lateral interaction between biosorbent metal ions on the surface of the biosorbent particles. Table 1 offers information on the linear form of the Freundlich isotherm. While the Temkin isotherm addresses the indirect effects of adsorbent-adsorbate interactions. The heat of biosorption for all molecular layers decreases linearly with coverage due to interactions between sorbents and sorbents.[98] However, the Dubinin-Radushkevich (D-R) isotherm is applied to estimate the pore-filling mechanism and predict the physical or chemical nature of the adsorption process. It is generally applied to express the adsorption mechanism through Gaussian energy distribution on a heterogeneous surface.[99] Table 1 provides the parameters and linear form of the Temkin and the Dubinin-Radushkevich models.

The relevance of the isotherm equations is evaluated by $R^2$. The Langmuir isotherm was further documented by analyzing the Langmuir equilibrium parameter ($R_L$), as outlined in Equation Table 1. The nature of the biosorption process is distinguished by the value, for example, unfavorable ($R_L > 1$), linear ($R_L = 1$), favorable ($0 < R_L < 1$), and irreversible ($R_L = 0$).[100] The obtained $R_L$ value indicated that individual metals and quaternary biosorption were favorable ($0 < R_L < 1$) for both *K. rhizophila* (single bacterium) and a consortium (three isolates) of *K. rhizophila*, *B. megaterium*, and *S. ginsenosidimutans*, as shown in Table 10.

The value of $1/n$ for the Freundlich isotherm model showed the probability of the isotherm, n means adsorption intensity. For example, irreversible ($1/n = 0$), Favorable ($0 < 1/n < 1$), and unfavorable ($1/n > 1$). The values of $1/n$ calculated for both *K. rhizophila* (single bacteria) and a consortium (three isolates) of *K. rhizophila* and *B. megaterium* and *S. ginsenosidimutans* were ($0 < 1/n < 1$), which means it favors the Freundlich isothermal model. The $R^2$ values (correlation coefficients) were applied to evaluate the fit of both isothermal models. The values were found to be higher than 0.98 for the Langmuir models and 0.94 for the Freundlich models, indicating that the isotherm interpretation data fit well with both models, as shown in Table 10. However, the fit was better suited for the Langmuir model than the Freundlich model for high $R^2$ values with the Langmuir model.[101]

Temkin and D-R isotherm models were investigated to provide additional information regarding the interaction between the metal cations and the living biomasses. The model assumes the binding energy of the sorption largely depends on the surface coverage.[102] However, the results showed that the Temkin model did not fit well with the

experimental results, with a low $R^2$ value of 0.885, as in copper. Description of biosorption onto a single bacterium and consortium: the values of correlation coefficients $R^2$ were lower compared with Langmuir and Freundlich isotherms, except for Cr with the consortium, which was 0.965 while $R^2$ was 0.916 with Freundlich. The results indicated a nonuniform distribution of binding energy arising due to the interaction of the metal molecules. The correlation coefficient $R^2$ obtained from the Temkin model, as shown in Table 10, depicts the non-applicability of this model in the explanation of these adsorption processes. The Temkin model ignores the high and low concentrations of the target pollutant compound in the liquid phase and presumes that adsorption is a multilayer process. The reduced values of the B Temkin constant revealed that the interactions between the biosorbents and the target molecule were weak, also sustaining the physisorption.[103]

The Dubinin-Radushkevich (D-R) isotherm assumes the adsorption takes place on a heterogeneous and porous surface.[104] The D-R model did not fit well with the adsorption data, having a relatively low $R^2$ value, except Cr adsorption onto the consortium. The values of the mean free energy $E$ of sorption in all cases are below 8 kJ/moL, which means that the adsorption process is a physical process. It was reported that if $E$ is between 8 and 16 kJ/mol, the adsorption type is explained by ion-exchange and chemical adsorption, while if $E$ lies within the range of 1-8 kJ/mol, the adsorption type is explained by Ven Der Wells for the physisorption processes.[105] From Table 10, it was suggested that the adsorption of the metal ions by the adsorbent is physisorption in nature. Based on the differences in correlation coefficients, the D-R isotherm could not describe the experimental data, unlike the Langmuir isotherm.

## 4.3 *Biosorption kinetics study*

The kinetic mechanism of biosorption was analyzed using pseudo-first-order, pseudo-second-order, Elovich model, and intra-particle diffusion. The pseudo-second-order model provided a good fit for the biosorption of all single metals, indicating chemisorption. However, it did not provide a good fit for a quaternary consortium. The pseudo-second-order model supports the validity of the biosorption of single and quaternary metals, indicating chemisorption. It has been stated that the pseudo-second-order kinetic model describes the adsorption of solute ions via cation exchange or chemical participation on the adsorbent surface, indicating that a chemical process is involved during the adsorption.[106] The results showed the pseudo-first-order model best describes quaternary indicating physisorption. It was reported that Pseudo-first-order generally denotes that physisorption is involved as the main mechanism instead of chemisorption. However, more evidence must be presented to prove that the mechanism is chemisorption. Such as the evaluation of energy and the process speeds in relation to the sizes of the adsorbent particles.[107]

The adsorption of metals may have involved both physisorption and chemisorption mechanisms as a result of earlier observations. The initial sorption rate ($h$) of single metals onto a single isolate was better for Cu, followed by Zn and Ni. As well, the initial sorption rates of Cu and quaternary were better on the consortium. This may be due to the ionic radius of the metal, which makes it difficult to diffuse to the surface of the adsorbents.[69] Furthermore, the amounts of single metals such as copper, zinc, and nickel were highly adsorbed in quaternary solutions by *K. rhizophila* and a consortium of three isolates, *B. megaterium*, *S. ginsenosidimutans*, and *K. rhizophila*, suggesting a negative synergistic interaction. Only the adsorption of chromium was slightly lower in the quaternary solution, indicating that the reaction was rather antagonistic.

In addition, electronegativity, which is another factor, affects the adsorption capacity because higher electronegativity produces stronger bonds with functional groups containing oxygen.[108] As was reported by Lo et al.,[69,109] the ionic properties of Ni, Cu, Zn, and Cr (VI) and their effect on biosorption can thus be observed. Small ionic radii to Ni (0.70 Å) and higher electronegativity (1.91); Cu and Zn were (0.72 Å) and (0.74 Å) and electronegativity (1.90) and (1.65). While a slower rate was obtained for Cr, despite its small ionic radius (0.52 Å) compared to other metals, the electronegativity was low (1.66).

## 4.4 *Biosorption thermodynamics*

The study evaluated the thermodynamic behaviour of single and quaternary metals on *K. rhizophila* and consortium biomass, focusing on changes in free energy, enthalpy, and entropy. Gibbs free energy changes ($\Delta G°$) were calculated for Cu, Zn, Ni, Cr, and quaternary biosorption at 25, 30, 37, 42, and 50 °C. The results illustrated negative values of $\Delta G°$ with all single metals and quaternary, which indicated the spontaneous nature, thermodynamic feasibility, and

preferential biosorption. The decrease in $\Delta G°$ values with an increase in temperature showed a decrease in the feasibility of biosorption at higher temperatures Cai and co-workers.[49] As well, the $\Delta H°$ parameters for metal biosorption of both single metals and quaternary metals appeared to be positive values, which indicated the endothermic nature of the biosorption process at 25-50 °C. The energy released in breaking a bond is less than the energy absorbed in making the bond in the endothermic process. As a result, this process is thought to have absorbed energy in the form of heat from its surroundings Abubakar et al.[40] Also, the results showed that $\Delta S°$ values for all metals were positive, which revealed the randomness of the adsorbates at the solid/solution interface during the binding of adsorbates to the active sites of the adsorbents and when the biosorption process occurred.[91]

The measured values of $\Delta G°$, $\Delta H°$, and $\Delta S°$, reflected the biosorption ability of metals individually and quaternary by *K. rhizophila* and a consortium of three isolates (*K. rhizophila*, *S. ginsenosidimutans*, and *B. megaterium*) and the nature of the biosorption process. The capacity for biosorption increased with temperature, indicating a spontaneous, feasible, and endothermic process with a negative Gibbs activation energy ($\Delta G°$) and positive enthalpy changes ($\Delta H°$), the latter indicating that the reaction consumes energy, and positive entropy values of ($\Delta S°$), indicating a random increase in the solid-solution interface and affinity bacteria for metal ions.

## 4.5 *Practical implications, difficulties, and suggestions of this study*

Conventional approaches to managing water and wastewater have several drawbacks, including high energy requirements, the production of secondary hazardous sludge, and operating expenses that are excessively costly for developing nations. For this purpose, the current study investigates the biosorption of heavy metals onto living microbes in multimetal-component systems compared to single metal component systems. Further research is necessary to close the gaps in the understanding of the biosorption ability of living bacteria in multimetal-component systems compared to single metal components, as well as the economic viability, biosorption system optimization, and desorption and regeneration of used biosorbents.

In addition, since real wastewater is a complex mixture of cations, anions, and compounds, it requires increased studies to understand the multicomponent adsorption of contaminants using biosorbents. Heavy metals are often found in multicomponent combinations in aquatic environments, making understanding the interaction of heavy metals and adsorbate molecules crucial for effective wastewater treatment.

Metal biosorption in multimetal-component systems faces challenges due to the existence of other competing heavy metal ions. The determination of biosorbent efficiency, possible practical applications, and reduction of heavy metals in multicomponent systems is crucial. Evaluating multicomponent adsorption from complex mixtures such as binary, ternary, quaternary, and quinary solutions using locally and naturally occurring materials like living biomass requires optimization of independent adsorption parameters. The multicomponent sorption of heavy metals is significantly influenced by these independent adsorption parameters, which include reaction duration, solution pH, agitation speed, adsorbent dose, initial metal ion concentration, ionic strength, and reaction temperature Additionally, applying multicomponent adsorption isotherms would confront competitive heavy metal sorption mechanisms; therefore, improving the physicochemical conditions for biosorbents and biosorption capacity is necessary.

The influence of different types of contaminants, such as inorganic chemicals, on each other, as well as the effect that varying initial concentrations of metal have on the biodegradation and biosorption of the contaminants, has also received little attention. For these reasons, it is now time for the authors to select the most advanced study in biosorption from multicomponent solutions for application from laboratory scale to experimental and/or industrial scale. Therefore, additional research should be conducted utilizing multicomponent biosorption isotherm models from significant investigations to comprehend the interactions between contaminants and decrease the antagonistic effects of one heavy metal on other heavy metal ions in these systems. Determine the combined effects of pollutants in aquatic environments as well.

The study demonstrates that indigenous bacteria, especially in consortium form, can improve the bioremediation of industrial pollutants in aquatic habitats, but there are challenges that may hinder metal bioremediation, such as heavy metal concentration, the toxicity of the metals to the bio remediators when in their living forms, and the potential success of the bacteria in pollutant processing in various environments.

## 5. Conclusions

Co-biosorption is a brand-new, highly developed technology that has been shown to have a high potential for the efficient removal of contaminants from effluents. The results of this study demonstrated the potential advantages of using living biomass to remove metal ions from aqueous media and their applicability depending on isotherms, kinetics, and thermodynamics. The best biosorption values of these metals were produced for both the individual isolate and the consortium at optimal conditions. The results found that living biomass, as a consortium rather than using a single biomass, was effectively able to remove mineral mixtures from electroplating effluent under precisely optimized conditions. It was also shown that for most metal-equilibrium and kinetic data, the Langmuir model and pseudo-second-order kinetic model provided a better fit. The spontaneous and endothermic nature of the process was confirmed by the thermodynamic parameters of the biosorption. This makes it a promising material for multimetal removal and bioremediation in polluted areas with low pH (weak acidity) or close to neutral pH and at low temperatures, as well as illustrating that the efficiency of living biomass in metal adsorption from multicomponent systems depends on parameters like contact time, pH, inoculation dosage, and initial metal ion concentration. These parameters and competitive adsorption mechanisms, such as synergistic, antagonistic, and non-reactive effects, must be considered when utilizing multicomponent sorption isotherm models.

## Availability of data and materials

The datasets generated during and/or analyzed during the current study are available from the corresponding author on reasonable request. All data generated or analyzed during this study are included in the present article.


## Funding

This study was sponsored by the Fundamental Research Grant Scheme (FRGS) [(KPT Reference Code: FRGS/1/2019/STG05/UPM/02/11) (Vote Number: 5540228) (Project Code: 01-01-19-2103FR)] awarded by the Ministry of Higher Education (MOHE), Malaysia.

## Acknowledgements

The authors would like to thank the laboratories of the Faculty of Forestry and Environment, Putra University, for providing the research facilities.


## Conflict of interest

The authors declare that they have no competing interests.

## References


[1] Olukanni, D. O.; Agunwamba, J. C.; Ugwu, E. I. Biosorption of heavy metals in industrial wastewater using micro-organisms (*Pseudomonas aeruginosa*). *Am. J. Sci. Ind. Res.* **2014,** *5*(2), 81-87.

[2] Singh, V.; Ram, C. Physico-chemical characterization of electroplating industrial effluents of Chandigarh and Haryana region. *J. Civil. Environ. Eng*. **2016,** *6*(4), 1-6.

[3] Liu, P.-C.; Vilando, A. C.; Lu, M.-C. Treatment of synthetic zinc and nickel wastewater and identification of its crystallization products by fluidized bed homogeneous crystallization technology. *Process Saf. Environ. Prot*. **2022,** *164*, 154-163.

[4] Hayati, B.; Maleki, A.; Najafi, F.; Gharibi, F.; McKay, G.; Gupta, V. K.; Harikaranahalli Puttaiah, S.; Marzban, N. Heavy metal adsorption using PAMAM/CNT nanocomposite from aqueous solution in batch and continuous fixed bed systems. *Chem. Eng. J.* **2018,** *346*, 258-270.
[5] Macena, M.; Pereira, H.; Cruz-Lopes, L.; Grosche, L.; Esteves, B. Competitive adsorption of metal ions by lignocellulosic materials: A review of applications, mechanisms and influencing factors. *Separations* **2025,** *12*(3), 70.
[6] Mahamadi, C. On the dominance of Pb during competitive biosorption from multi-metal systems: A review. *Cogent Environ. Sci.* **2019,** *5*(1), 1635335.
[7] Ordóñez, J. I.; Cortés, S.; Maluenda, P.; Soto, I. Biosorption of heavy metals with algae: Critical review of its application in real effluents. *Sustainability* **2023,** *15*, 5521.
[8] Carreira, A. R. F.; Passos, H.; Coutinho, J. A. P. Metal biosorption onto non-living algae: A critical review on metal recovery from wastewater. *Green Chem*. **2023,** *25*(15), 5775-5788.
[9] Pagnucco, G.; Overfield, D.; Chamlee, Y.; Shuler, C.; Kassem, A.; Opara, S.; Najaf, H.; Abbas, L.; Coutinho, O.; Fortuna, A.; Sulaiman, F.; Farinas, J.; Schittenhelm, R.; Catalfano, B.; Li, X.; Tiquia-Arashiro, S. M. Metal tolerance and biosorption capacities of bacterial strains isolated from an urban watershed. *Front. Microbiol*. **2023,** *14*, 1278886.
[10] Muhammad, A.; Rodhi, M. N. M.; Hamid, K. H. K. In *Comparison biosorption of heavy metal ions from single and multi metal synthetic solution by living Pleurotus ostreatus*, 2012 IEEE Colloquium on Humanities, Science and Engineering (CHUSER); IEEE, 2012; pp 846-849.
[11] Yu, Z.; Han, H.; Feng, P.; Zhao, S.; Zhou, T.; Kakade, A.; Kulshrestha, S.; Majeed, S.; Li, X. Recent advances in the recovery of metals from waste through biological processes. *Bioresour. Technol.* **2020,** *297*, 122416.
[12] Hu, S.; Wei, Z.; Liu, T.; Zuo, X.; Jia, X. Adsorption of $Hg^{2+}$/$Cr^{6+}$ by metal-binding proteins heterologously expressed in *Escherichia coli*. *BMC Biotechnol.* **2024,** *24*(1), 15.
[13] Karnwal, A. Unveiling the promise of biosorption for heavy metal removal from water sources. *Desalin. Water Treat*. **2024,** *319*, 100523.
[14] M.; Hlihor, R.; Cozma, P.; Simion, I.; Apostol, M.; Gavrilescu, M. Sustainable application of biosorption and bioaccumulation of persistent pollutants in wastewater treatment: Current practice. *Processes* **2021,** *9*(10), 1696.
[15] Acosta, I.; Rodríguez, A.; Cárdenas, J. F.; Martínez, V. M. Biosorption of mercury from aqueous solutions by biosorbents. In *Mercury Toxicity*; Kumar, N., Ed.; Springer Nature Singapore: Singapore, 2023; pp 357-374.
[16] Ljubic, V.; Perendija, J.; Cvetkovic, S.; Rogan, J.; Trivunac, K.; Stojanovic, M.; Popovic, M. Removal of $Ni^{2+}$ ions from contaminated water by new exopolysaccharide extracted from *K. oxytoca* J7 as biosorbent. *J. Polym. Environ.* **2024,** *32*(3), 1105-1121.
[17] Bangaraiah, P. Optimization of multimetal adsorption by acid-treated Fabaceae biosorbent: Kinetics and equilibrium. *Biomass Conv. Bioref.* **2023,** *13*(16), 15235-15250.
[18] Bind, A.; Kushwaha, A.; Devi, G.; Goswami, S.; Sen, B.; Prakash, V. Biosorption valorization of floating and submerged macrophytes for heavy-metal removal in a multi-component system. *Appl. Water Sci.* **2019,** *9*(4), 95.
[19] Mosa, K. A.; Saadoun, I.; Kumar, K.; Helmy, M.; Dhankher, O. P. Potential biotechnological strategies for the cleanup of heavy metals and metalloids. *Front. Plant Sci*. **2016,** *7*, 303.
[20] Kumar, L.; Bharadvaja, N. Microbial remediation of heavy metals. In *Microbial Bioremediation & Biodegradation*; Shah, M. P., Ed.; Springer Singapore: Singapore, 2020; pp 49-72.
[21] Roy, A. S.; Hazarika, J.; Manikandan, N. A.; Pakshirajan, K.; Syiem, M. B. Heavy metal removal from multicomponent system by the cyanobacterium Nostoc muscorum: Kinetics and interaction study. *Appl. Biochem. Biotechnol.* **2015,** *175*(8), 3863-3874.
[22] Costa, F.; Tavares, T. Biosorption of multicomponent solutions: A state of the art of the understudy case. In *Biosorption*; Derco, J., Vrana, B., Eds.; InTech: Rijeka, 2018.
[23] De Morais França, A. M.; Sousa, F. W.; Loiola, A. R.; De Luna, F. M. T.; Vidal, C. B.; Do Nascimento, R. F. Study of $Cu^{2+}$, $Ni^{2+}$, and $Zn^{2+}$ competitive adsorption on synthetic zeolite: An experimental and theoretical approach. *Desalin. Water Treat*. **2021,** *227*, 263-277.
[24] Girish, C. R. Simultaneous adsorption of pollutants onto the adsorbent: Review of interaction mechanism between the pollutants and the adsorbent. *Int. J. Eng. Technol.* **2018,** *7*(4), 3613-3622.
[25] Singh, N.; Balomajumder, C. Equilibrium isotherm and kinetic studies for the simultaneous removal of phenol and cyanide by use of *S. odorifera* (MTCC 5700) immobilized on coconut shell activated carbon. *Appl. Water Sci.* **2017,** *7*(6), 3241-3255.
[26] Wierzba, S. Biosorption of lead(II), zinc(II) and nickel(II) from industrial wastewater by *Stenotrophomonas*

*maltophilia* and *Bacillus subtilis*. *Pol. J. Chem. Technol.* **2015,** *17*(1), 79-87.
[27] Rasmey, A.-H.; Aboseidah, A.; Youssef, A. Phenotypic and molecular characterization of a novel isolate of *Pseudomonas aeruginosa* applicable for biosorption of $Pb^{2+}$ from waste water: Application of biosorption isotherm models. *Egypt. J. Microbiol*. **2018**.
[28] Torres, E. Biosorption: A review of the latest advances. *Processes* **2020,** *8*(12), 1584.
[29] Bayuo, J.; Rwiza, M. J.; Sillanpää, M.; Mtei, K. M. Removal of heavy metals from binary and multicomponent adsorption systems using various adsorbents - A systematic review. *RSC Adv*. **2023,** *13*(19), 13052-13093.
[30] Uwamariya, V. *Adsorptive Removal of Heavy Metals from Groundwater by Iron Oxide Based Adsorbents*; CRC Press: Leiden, 2013; pp 152.
[31] Adnan, N. A.; Halmi, M. I. E.; Abd Gani, S. S.; Zaidan, U. H.; Abd Shukor, M. Y. Comparison of joint effect of acute and chronic toxicity for combined assessment of heavy metals on *Photobacterium* sp. NAA-MIE. *Int. J. Environ. Res. Public Health* **2021,** *18*(12), 6644.
[32] Michalak, I.; Chojnacka, K.; Witek-Krowiak, A. State of the art for the biosorption process—A review. *Appl. Biochem. Biotechnol.* **2013,** *170*(6), 1389-1416.
[33] Xie, P.; Hao, X.; Mohamad, O. A.; Liang, J.; Wei, G. Comparative study of chromium biosorption by *Mesorhizobium amorphae* strain CCNWGS0123 in single and binary mixtures. *Appl. Biochem. Biotechnol*. **2013,** *169*(2), 570-587.
[34] Al-Rub, F. A. A.; El-Naas, M. H.; Ashour, I.; Al-Marzouqi, M. Biosorption of copper on *Chlorella vulgaris* from single, binary and ternary metal aqueous solutions. *Process Biochem*. **2006,** *41*(2), 457-464.
[35] Fomina, M.; Gadd, G. M. Biosorption: Current perspectives on concept, definition and application. *Bioresour. Technol.* **2014,** *160*, 3-14.
[36] Michalak, I.; Chojnacka, K. The new application of biosorption properties of *Enteromorpha prolifera*. *Appl. Biochem. Biotechnol.* **2010**, *160*(5), 1540-1556.
[37] Kumar, A.; Bisht, B. S.; Joshi, V. D. Bioremediation potential of three acclimated bacteria with reference to heavy metal removal from waste. *Int. J. Environ. Sci* **2011,** *2*(2), 896-908.
[38] Abd El Hameed, A. H.; Eweda, W. E.; Abou-Taleb, K. A. A.; Mira, H. I. Biosorption of uranium and heavy metals using some local fungi isolated from phosphatic fertilizers. *Ann. Agric. Sci.* **2015,** *60*(2), 345-351.
[39] Alhammadi, E.; Halimoon, N.; Johari, W. L. W.; Zulkeflee, Z. Potentially applicable bioremediation mechanisms for metal-tolerant bacteria from industrial waste electroplating. *Int. J. Environ. Sci. Technol*. **2024,** *21*(5), 4817-4836.
[40] Bergey, D. H.; Holt, J. G. *Bergey's Manual of Systematic Bacteriology, 1st Ed*.; Williams & Wilkins: Baltimore, 1989.
[41] Benmalek, Y.; Fardeau, M.-L. Isolation and characterization of metal-resistant bacterial strain from wastewater and evaluation of its capacity in metal-ions removal using living and dry bacterial cells. *Int. J. Environ. Sci. Technol.* **2016,** *13*(9), 2153-2162.
[42] Burnley, L. E. Heavy Metal Resistance in the Genus Gluconobacter. Master's Thesis, Virginia Polytechnic Institute and State University: Blacksburg, VA, USA, 2000.
[43] Pandit, R. J.; Patel, B.; Kunjadia, P. D.; Nagee, A. Isolation, characterization and molecular identification of heavy metal resistant bacteria from industrial effluents, Amala-Khadi-Ankleshwar, Gujarat. *Int. J. Environ. Sci*. **2013,** *3*(5), 1689-1699.
[44] Jaafar, R.; Al-Sulami, A.; Al-Taee, A.; Aldoghachi, F.; Napes, S. Biosorption and bioaccumulation of some heavy metals by *Deinococcus radiodurans* isolated from soil in Basra Governorate-Iraq. *J. Biotechnol. Biomater*. **2015,** *5*(2), 190.
[45] Fadel, M.; Hassanein, N. M.; Elshafei, M. M.; Mostafa, A. H.; Ahmed, M. A.; Khater, H. M. Iosorption of manganese from groundwater by biomass of *Saccharomyces cerevisiae*. *HBRC J*. **2017,** *13*(1), 106-113.
[46] Murthy, S.; Bali, G.; Sarangi, S. K. Effect of lead on growth, protein and biosorption capacity of *Bacillus cereus* isolated from industrial effluent. *J. Environ. Biol*. **2014,** *35*(2), 407-114.
[47] Cui, H.; Yan, C.; Jia, P.; Cao, W. Adsorption and sensing behaviors of $SF_6$ decomposed species on Ni-doped $C_3N$ monolayer: A first-principles study. *Appl. Surf. Sci.* **2020,** *512*, 145759.
[48] Abdulaziz, M.; Musayev, S. Multicomponent biosorption of heavy metals from aqueous solutions: A review. *Pol. J. Environ. Stud*. **2017,** *26*(4), 1433-1441.
[49] Langmuir, I. The constitution and fundamental properties of solids and liquids. *Part I. Solids. J. Am. Chem. Soc.* **1916,** *38*(11), 2221-2295.
[50] Cai, Y.; Li, X.; Liu, D.; Xu, C.; Ai, Y.; Sun, X.; Zhang, M.; Gao, Y.; Zhang, Y.; Yang, T.; Wang, J.; Wang, L.; Li, X.;

Yu, H. A novel Pb-resistant *Bacillus subtilis* bacterium isolate for co-biosorption of hazardous Sb(III) and Pb(II): Thermodynamics and application strategy. *Int. J. Environ. Res. Public Health* **2018,** *15*(4), 702.
[51] Thilagavathy, P.; Santhi, T.; Manonmani, S. Biosorption of cobalt(II) by Acacia nilotica from single and multicomponent systems of aqueous solution: Equilibrium, isotherm, kinetic and thermodynamic studies. *Glob. J. Biol. Agric. Health Sci.* **2014,** *3*(3), 194-202.
[52] Eloussaief, M.; Benzina, M. Efficiency of natural and acid-activated clays in the removal of Pb(II) from aqueous solutions. *J. Hazard. Mater*. **2010,** *178*(1-3), 753-757.
[53] Freundlich, H. Über die adsorption in lösungen [On adsorption in solutions]. *Z. Phys. Chem*. **1907,** *57U*(1), 385-470.
[54] Jin, Y.; Luan, Y.; Ning, Y.; Wang, L. Effects and mechanisms of microbial remediation of heavy metals in soil: A critical review. *Appl. Sci*. **2018,** *8*(8), 1336.
[55] Temkin, M. J.; Pyzhev, V. Recent modifications to Langmuir isotherms. *Acta Physicochim. USSR* **1940,** *12*, 217-222.
[56] Imran Din, M.; Mirza, M. L.; Ata, S.; Athar, M.; Mohsin, I. U. Thermodynamics of biosorption for removal of Co(II) ions by an efficient and ecofriendly biosorbent (*Saccharum bengalense*): Kinetics and isotherm modeling. *Journal of Chemistry* **2013,** *2013*(1), 528542.
[57] Dubinin, M. M. The potential theory of adsorption of gases and vapors for adsorbents with energetically nonuniform surfaces. *Chem. Rev.* **1960,** *60*(2), 235-241.
[58] Radushkevich, L. V. Potential theory of sorption and structure of carbons. *Russ. J. Phys. Chem*. **1949,** *23*(12), 1410-1420.
[59] Ragadhita, R.; Nandiyanto, A. B. D. How to calculate adsorption isotherms of particles using two-parameter monolayer adsorption models and equations. *Indonesian J. Sci. Technol*. **2021,** *6*(1), 205-234.
[60] Abubakar, A.; Sabo, I. A.; Yahuza, S. Thermodynamics modelling of lead (II) biosorption using *Cystoseira stricta* biomass. *Bioremed. Sci. Technol. Res*. **2020,** *8*(2), 21-23.
[61] Sahmoune, M. N. Evaluation of thermodynamic parameters for adsorption of heavy metals by green adsorbents. *Environ. Chem. Lett*. **2019,** *17*(2), 697-704.
[62] Hajahmadi, Z.; Younesi, H.; Bahramifar, N.; Khakpour, H.; Pirzadeh, K. Multicomponent isotherm for biosorption of Zn(II), Co(II) and Cd(II) from ternary mixture onto pretreated dried *Aspergillus niger* biomass. *Water Resour. Ind*. **2015,** *11*, 71-80.
[63] Liu, Y.; Fan, T.; Zeng, G.; Li, X.; Tong, Q.; Ye, F.; Zhou, M.; Xu, W.; Huang, Y. Removal of cadmium and zinc ions from aqueous solution by living *Aspergillus niger*. *Trans. Nonferrous Met. Soc. China* **2006,** *16*(3), 681-686.
[64] Aharoni, C.; Kinetics of activated chemisorption. Part 2.—Theoretical models. *J. Chem. Soc., Faraday Trans.* **1977,** *73*, 456.
[65] Zhou, X. Correction to the calculation of Polanyi potential from Dubinin-Radushkevich equation. *J. Hazard. Mater.* **2020,** *384*, 121101.
[66] Amrutha, N.; Jeppu, G.; Girish, C. R.; Prabhu, B.; Mayer; K. Multi-component adsorption isotherms: Review and modelling studies. *Environ. Process.* **2023,** *10*(2), 38.
[67] Lagergren, S. Zur theorie der sogenannten adsorption gelöster Stoffe [On the theory of so-called adsorption of dissolved substances]. *Z. Chem. Ind. Kolloide*. **1907,** *2*, 15.
[68] Ghaed, S.; Shirazi, E. K. Biosorption of copper ions by Bacillus and Aspergillus species. *Adsorpt. Sci. Technol.* **2013,** *31*(10), 869-890.
[69] Eluke, L. O.; Ajiwe, V.; Akpomie, K.; Ho, C. O. Biosorption kinetics and isotherm investigation of Co(II), Zn(II) and Pb(II) ions on gourd cell seed husk adsorbent. *Der Pharma Chem.* **2017,** *9*(11), 44-55.
[70] Godwin, O.; Ogbeide, O. M; Ezeh, E. C.; Chukwuekeh. J. I.; Nwankwo, O. D.; Igwilo, C. N. Kinetic and thermodynamic studies on adsorption of lead (II) ions from aqueous solutions using polymer-modified coconut shell activated carbon (MCSAC). *Int. J. Chem. Sci.* **2020,** *4*(1), 1-8.
[71] Jannat Abadi, M. H.; Nouri, S. M. M.; Zhiani, R.; Heydarzadeh, H. D.; Motavalizadehkakhky, A. Removal of tetracycline from aqueous solution using Fe-doped zeolite. *Int. J. Ind. Chem*. **2019,** *10*(4), 291-300.
[72] Din, M. I.; Hussain, Z.; Mirza, M. L.; Shah, A. T.; Athar, M. M. Adsorption optimization of lead (II) using *Saccharum bengalense* as a non-conventional low cost biosorbent: Isotherm and thermodynamics modeling. *Int. J. Phytoremediation* **2014,** *16*(9), 889-908.
[73] Dadrasnia, A.; Chuan Wei, K.; Shahsavari, N.; Azirun, M.; Ismail, S. Biosorption potential of Bacillus salmalaya strain 139SI for removal of Cr(VI) from aqueous solution. *Int. J. Environ. Res. Public Health* **2015,** *12*(12), 15321-15338.

[74] Edet, U. A.; Ifelebuegu, A. O. Kinetics, isotherms, and thermodynamic modeling of the adsorption of phosphates from model wastewater using recycled brick waste. *Processes* **2020,** *8*(6), 665.
[75] Mathivanan, K.; Chandirika, J. U.; Vinothkanna, A.; Yin, H.; Liu, X.; Meng, D. Bacterial adaptive strategies to cope with metal toxicity in the contaminated environment - A review. *Ecotoxicol. Environ. Saf.* **2021,** *226*, 112863.
[76] Clarridge, J. E. Impact of 16S rRNA gene sequence analysis for identification of bacteria on clinical microbiology and infectious diseases. *Clin. Microbiol. Rev*. **2004,** *17*, 840-862.
[77] Schlaberg, R.; Simmon, K. E.; Fisher, M. A. A systematic approach for discovering novel, clinically relevant bacteria. *Emerg. Infect. Dis.* **2012,** *18*(3), 422-430.
[78] Banerjee, A.; Jhariya, M. K.; Yadav, D. K.; Raj, A. Micro-remediation of metals: A new frontier in bioremediation. In *Handbook of Environmental Materials Management*; Hussain, C. M., Ed.; Springer International Publishing: Cham, 2018; pp 1-36.
[79] Alotaibi, B. S.; Khan, M.; Shamim, S. Unraveling the underlying heavy metal detoxification mechanisms of Bacillus species. *Microorganism*s **2021,** *9*(8), 1628.
[80] Afridi, M. S.; Van Hamme, J. D.; Bundschuh, J.; Sumaira; Khan, M. N.; Salam, A.; Waqar, M.; Munis, M. F. H.; Chaudhary, H. J. Biotechnological approaches in agriculture and environmental management - Bacterium *Kocuria rhizophila* 14ASP as heavy metal and salt-tolerant plant growth-promoting strain. *Biologia* **2021,** *76*(10), 3091-3105.
[81] Feruke-Bello, Y. M.; Babalola, G.; Odeyemi, O. A comparative study of the wild and mutated heavy metal resistant *Klebsiella variicola* generated for cadmium bioremediation. *Bioremediation J*. **2018,** *22*, 28-42.
[82] Ishida, T. Antibacterial mechanism of $Ag^{+}$ ions for bacteriolyses of bacterial cell walls via peptidoglycan autolysins, and DNA damages. *MOJ Toxicol*. **2018,** *4*(5), 345-350.
[83] Mulik, A. R; Kulkarni, P.; Bhadekar, R. K. Biosorption studies on nickel and chromium by *Kocuria* sp. BRI 36 biomass. *Int. J. Appl. Eng. Res*. **2018,** *13*(9), 6886-6893.
[84] Pham, V. H. T.; Kim, J.; Chang, S.; Chung, W. Investigation of lipolytic-secreting bacteria from an artificially polluted soil using a modified culture method and optimization of their lipase production. *Microorganisms* **2021,** *9*(12), 2590.
[85] Desoky, E.-S. M.; Merwad, A.-R. M.; Semida, W. M.; Ibrahim, S. A.; El-Saadony, M. T.; Rady, M. M. Heavy metals-resistant bacteria (HM-RB): Potential bioremediators of heavy metals-stressed Spinacia oleracea plant. *Ecotoxicol. Environ. Saf*. **2020,** *198*, 110685.
[86] Verma, S.; Kuila, A. Bioremediation of heavy metals by microbial process. *Environ. Technol. Innovation* **2019,** *14*, 100369.
[87] Haq, F.; Butt, M.; Ali, H.; Chaudhary, H. J. Biosorption of cadmium and chromium from water by endophytic *Kocuria rhizophila*: Equilibrium and kinetic studies. *Desalin. Water Treat.* **2016,** *57*(42), 19946-19958.
[88] Yahuza, S.; Sabo, I. A.; Abubakar, A.; Shukor, M. Y. Biosorption of lead (II) ions by brown algae: A thermodynamic study. *Bull. Environ. Sci. Sust. Manage* **2020,** *4*(2), 1-5.
[89] Fathollahi, A.; Khasteganan, N.; Coupe, S. J.; Newman, A. P. A meta-analysis of metal biosorption by suspended bacteria from three phyla. *Chemosphere* **2021,** *268*, 129290.
[90] Che Sulaiman, I. S.; Basri, M.; Fard Masoumi, H. R.; Chee, W. J.; Ashari, S. E.; Ismail, M. Effects of temperature, time, and solvent ratio on the extraction of phenolic compounds and the anti-radical activity of Clinacanthus nutans Lindau leaves by response surface methodology. *Chem. Cent. J.* **2017,** *11*(1), 54.
[91] Sayyadi, S.; Ahmady-Asbchin, S.; Kamali, K.; Tavakoli, N. Thermodynamic, equilibrium and kinetic studies on biosorption of $Pb^{2+}$ from aqueous solution by *Bacillus pumilus* sp. AS1 isolated from soil at abandoned lead mine. *J. Taiwan Inst. Chem. Eng*. **2017,** *80*, 701-708.
[92] Medfu Tarekegn, M.; Zewdu Salilih, F.; Ishetu, A. I. Microbes used as a tool for bioremediation of heavy metal from the environment. *Cogent Food Agric*. **2020,** *6*(1), 1783174.
[93] Keshtkar, A. R.; Mohammadi, M.; Moosavian, M. A. Equilibrium biosorption studies of wastewater U(VI), Cu(II) and Ni(II) by the brown alga *Cystoseira indica* in single, binary and ternary metal systems. *J. Radioanal. Nucl. Chem*. **2015,** *303*(1), 363-376.
[94] Eletta, O. A. A.; Ayandele, F. O.; Ighalo, J. O. Adsorption of Pb(II) and Fe(II) by mesoporous composite activated carbon from Tithonia diversifolia stalk and Theobroma cacao pod. *Biomass Conv. Bioref*. **2023,** *13*(11), 9831-9840.
[95] Kul, S. Removal of Cu(II) from aqueous solutions using modified sewage sludge ash. *Int. J. Environ. Sci. Technol*. **2021,** *18*(12), 3795-3806.
[96] Girish, C. R. Various isotherm models for multicomponent adsorption: A review. *Int. J. Civil Eng. Technol.* **2019,** *8*(10), 80-86.

[97] El-Amier, Y. A.; Elsayed, A.; El-Esawi, M. A.; Noureldeen, A.; Darwish, H.; Fakhry, H. Optimizing the biosorption behavior of *Ludwigia stolonifera* in the removal of lead and chromium metal ions from synthetic wastewater. *Sustainability* **2021,** *13*(11), 6390.
[98] Cheng, Q.; Fang, Z.; Yi, X.; An, X.; Tang, B.; Xu, Y. "Ex situ" concept for toughening the RTmable BMI matrix composites, part I: Improving the interlaminar fracture toughness. *J. Appl. Polym. Sci.* **2008,** 109.
[99] Khan, Z.; Rehman, A.; Hussain, S. Z.; Nisar, M. A.; Zulfiqar, S.; Shakoori, A. R. Cadmium resistance and uptake by bacterium, Salmonella enterica 43C, isolated from industrial effluent. *AMB Express* **2016,** *6*(1), 54.
[100]Jaafar, A.; Darchen, A.; Hamzi, S. E.; Lakbaibi, Z.; Driouich, A.; Boussaoud, A.; Yaacoubi, A.; El Makhfouk, M.; Hachkar, M. Optimization of cadmium ions biosorption by fish scale from aqueous solutions using factorial design analysis and Monte Carlo simulation studies. *J. Environ. Chem. Eng*. **2021,** *9*(1), 104727.
[101]Gupta, V. K.; Rastogi, A. Biosorption of lead from aqueous solutions by green algae *Spirogyra* species: Kinetics and equilibrium studies. *J. Hazard. Mater.* **2008,** *152*(1), 407-414.
[102]Elebo, A., Ekwumemgbo, P. A.; Elaoyi, D. P.; Jibunor, V. U.; Areguamen, O. I. Isotherm and kinetic investigations of toxic metal decontamination from biofluid by untreated biosorbent using a Batch design. *J. Chem. Lett.* **2023,** *4*(2), 71-80.
[103]Rusu, L.; Grigoraş, C.-G.; Simion, A.-I.; Suceveanu, E.-M.; Istrate, B.; Harja, M. Biosorption potential of microbial and residual biomass of *Saccharomyces pastorianus* immobilized in calcium alginate matrix for pharmaceuticals removal from aqueous solutions. *Polymers* **2022,** *14*, 2855.
[104]Al-Ghouti, M. A.; Da'ana, D. A. Guidelines for the use and interpretation of adsorption isotherm models: A review. *J. Hazard. Mater.* **2020,** *393*, 122383.
[105]Mobasherpour, I.; Salahi, E.; Ebrahimi, M. Thermodynamics and kinetics of adsorption of Cu(II) from aqueous solutions onto multi-walled carbon nanotubes. *J. Saudi Chem. Soc.* **2014,** *18*(6), 792-801.
[106]Al-Harby, N. F.; Albahly, E. F.; Mohamed, N. A. Kinetics, isotherm and thermodynamic studies for efficient adsorption of Congo red dye from aqueous solution onto novel cyanoguanidine-modified chitosan adsorbent. *Polymers* **2021,** *13*(24), 4446.
[107]Abd Wahab Sha'arani, S.; Ros Saidon Khudri, M. A. M.; Othman, A. R.; Halmi, M. I. E.; Yasid, N. A.; Shukor, M. Y. Kinetic analysis of the adsorption of the brominated flame retardant 4-bromodiphenyl ether onto biochar-immobilized *Sphingomonas* sp. *Bioremed. Sci. Technol. Res.* **2019,** *7*(1), 8-12.
[108]Alexandre, P. *Practical Geochemistry*; Springer: Cham, Switzerland, 2021.
[109]Jain, M.; Garg, V. K.; Kadirvelu, K.; Sillanpää, M. Adsorption of heavy metals from multi-metal aqueous solution by sunflower plant biomass-based carbons. *Int. J. Environ. Sci. Technol*. **2016,** *13*(2), 493-500.